

## Genetic Disorders of Glycosylation

# Dissecting the transcriptional program of phosphomannomutase 2-deficient cells: Lymphoblastoid B cell lines as a valuable model for congenital disorders of glycosylation studies

Antonio Parrado<sup>2</sup>, Gonzalo Rubio<sup>3</sup>, Mercedes Serrano<sup>4</sup>,  
María Eugenia De la Morena-Barrio<sup>5</sup>, Salvador Ibáñez-Micó<sup>6</sup>,  
Natalia Ruiz-Lafuente<sup>2</sup>, Reinhard Schwartz-Albiez<sup>7</sup>, Ana Esteve-Solé<sup>8</sup>,  
Laia Alsina<sup>8</sup>, Javier Corral<sup>5</sup>, and Trinidad Hernández-Caselles<sup>3,1</sup>

<sup>2</sup>Immunology Service, Virgen de la Arrixaca University Clinic Hospital, IMIB-Arrixaca, 30120 Murcia, Spain, <sup>3</sup>Department of Biochemistry and Molecular Biology (B) and Immunology, Universidad de Murcia, IMIB-Arrixaca, 30120 Murcia, Spain, <sup>4</sup>Department of Pediatric Neurology, Institute of Pediatric Research-Hospital Sant Joan de Déu, U-703 Center for Biomedical Research on Rare Diseases, CIBERER, 08950 Esplugues de Llobregat, Barcelona, Spain, <sup>5</sup>Servicio de Hematología y Oncología Médica, Hospital Universitario Morales Meseguer, Centro Regional de Hemodonación, Universidad de Murcia, IMIB-Arrixaca, CIBERER, 30003 Murcia, Spain, <sup>6</sup>Pediatric Neurology Unit, Virgen de la Arrixaca University Clinic Hospital, 30120 Murcia, Spain, <sup>7</sup>CLS Cell Line Service BmbH, 69214 Eppelheim, Germany, and <sup>8</sup>Clinical Immunology and Primary Immunodeficiencies Unit, Pediatric Allergy and Clinical Immunology Department, Hospital Sant Joan de Déu, 08950 Esplugues de Llobregat, Barcelona, Spain

<sup>1</sup>To whom correspondence should be addressed: Tel: +34-868-887951; e-mail: trini@um.es

Received 10 May 2020; Revised 30 July 2021; Accepted 9 August 2021

### Abstract

Congenital disorders of glycosylation (CDG) include 150 disorders constituting in genetically and clinically heterogeneous diseases, showing significant glycoprotein hypoglycosylation that leads to pathological consequences on multiple organs and systems whose underlying mechanisms are not yet understood. A few cellular and animal models have been used to study specific CDG characteristics, although they have given limited information due to the few CDG mutations tested and the still missing comprehensive molecular and cellular basic research. Here, we provide specific gene expression profiles, based on ribonucleic acid (RNA) microarray analysis, together with some biochemical and cellular characteristics of a total of nine control Epstein–Barr virus-transformed lymphoblastoid B cell lines (B-LCL) and 13 CDG B-LCL from patients carrying severe mutations in the phosphomannomutase 2 (*PMM2*) gene, strong serum protein hypoglycosylation and neurological symptoms. Significantly dysregulated genes in *PMM2*-CDG cells included those regulating stress responses, transcription factors, glycosylation, motility, cell junction and, importantly, those related to development and neuronal differentiation and synapse, such as carbonic anhydrase 2 (CA2) and ADAM23. *PMM2*-CDG-associated biological consequences involved the unfolded protein response, RNA metabolism and the endoplasmic reticulum, Golgi apparatus and mitochondria components. Changes in the transcriptional and CA2 protein levels are consistent with the CDG physiopathology. These results demonstrate the global transcriptional impact in phosphomannomutase 2-deficient cells, reveal CA2 as a potential cellular biomarker and confirm B-LCL as an advantageous model for CDG studies.

**Key words:** B-lymphoblastoid cells, CA2, congenital disorders of glycosylation, gene expression profile, PMM2-CDG

## Introduction

Glycosylation is an important modification, which is essential for multiple biological processes that affect proteins and sphingolipids. Protein glycosylation represents a co- and post-translational process that is accomplished by an extensive and complex metabolic pathway that comprises three major stages which involve the synthesis of dolichol-linked oligosaccharides at the cytoplasmic side and in the lumen of the endoplasmic reticulum (ER), its attachment to proteins in the ER and the glycan remodeling in the ER and Golgi apparatus (GA). Genetic disorders impairing any step of this process give rise to a group of pathologies named congenital disorders of glycosylation (CDG). Currently, CDG represents a group of over 150 types of clinically and genetically heterogeneous disorders affecting multiple organ systems whose clinical presentations include neurologic, gastrointestinal, hepatic, cardiac, renal, hematologic, immunologic and skeletal abnormalities (Péanne et al. 2018; Altassan et al. 2019; Verheijen et al. 2019). The most common CDG type is PMM2-CDG (previously named CDG-1a), a type-I CDG caused by recessive pathogenic variants in the phosphomannomutase 2 (*PMM2*) genes. A deficient *PMM2* activity, which leads to the reduced conversion of mannose-6-P to mannose-1-P, results in low levels of guanosine 5'-diphospho-D-mannose (GDP-Man), a nucleotide-activated sugar that is essential for the elongation of the dolichol-bound oligosaccharide precursor (Shang et al. 2002). The intermediate consequence is a significant N-glycoprotein hypoglycosylation which may have pathological consequences by at least three different mechanisms: (a) protein hypoglycosylation causing incorrect folding and accumulation in the ER and subsequent degradation, (b) loss of function due to either the reduced levels of the protein (at least at the physiological localization) or to a lesser activity and (c) gain of function effect, such as acquiring new roles related to a differential specificity of interaction.

Drug-induced inhibition of glycosylation in cellular models results in the accumulation of misfolded proteins in the ER, which induces a complex protective reaction known as the unfolded protein response (UPR). In summary, the UPR is initiated and regulated by the ER stress sensors, IRE1, PERK and ATF6, which activate translational repression, transcriptional activation of ER chaperones, such as protein disulfide isomerases (PDIs), and the ER-associated degradation (ERAD) pathways to inhibit novel protein synthesis and to promote the folding and removal of unfolded proteins. The UPR shifts signaling from the protective pathway to the apoptotic pathway under excess or chronic ER stress to eliminate unhealthy cells (recently reviewed by Sicari et al. 2019). Related to these facts, CDG condition is considered as a form of chronic ER stress and UPR that is poorly studied.

Several research groups tried to dissect the CDG condition at cellular level by testing in vitro-cultured patient's fibroblast as CDG almost unique cellular model. Thus, in CDG-1 fibroblasts, accumulation of shortened lipid-linked oligosaccharide (LLO) was found, leading to a mild form of chronic ER stress in which LLO extension was continuously stress-activated (Shang et al. 2002). Other aspects of the UPR, such as expression of Bip/GRP78 and calreticulin ER chaperone proteins, were found unchanged. More recently, Lecca and collaborators, analyzing gene expression profile, reported a moderate

UPR in CDG-I fibroblasts compared to the UPR displayed by healthy cells treated with tunicamycin, which specifically inhibits the first step of N-linked glycosylation by inhibiting a N-acetylglucosamine transferase in the ER (Lecca et al. 2005, 2011). They reported a strong transcriptional increase of the *DNAJC3/P58IPK* gene and the expression of several chaperone proteins, including ERP70/PDIA4, calreticulin and members of the HSP40 family in patient's fibroblasts. The same transcriptomic and the subsequent protein analysis (Lecca et al. 2011) revealed a strong induction of gene encoding extracellular matrix components (*COMP*, *IGFBP5*, biglycan and collagen type I). These unique works were performed on a pool of three different types of CDG-I patients: four ALG6-CDG, three DPM1-CDG and two ALG12-CDG (with pathogenic mutations in *ALG6*, *DPM1* and *ALG12*, respectively) and, accordingly, their findings could be interpreted as part of the fibroblast UPR.

Distinct to fibroblast's studies, induced pluripotent stem cells (iPSCs), derived from a sole PMM2-CDG-patient fibroblasts, have been generated as a model of CDG cell differentiation and in vitro drug screening tests (Thiesler et al. 2016). Up-regulation of Nrf2 and some of its targets genes have been found on the zebrafish animal model of hypomorphic *pmm2* mutation (Mukaigasa et al. 2018), which is not related to human *PMM2* mutations. Besides CDG fibroblasts or zebrafish, some other animal models bearing a specific mutation are being developed (Chan et al. 2016; Parkinson et al. 2016). However, only few specific CDG mutations expressed on restricted genetic background animal models can be tested in these models, giving limited information. Consequently, patient's derived new cellular models are needed to find out more specific cellular and molecular characteristic to identify the CDG disorders.

Despite the amount of genetic and biochemical studies performed, the underlying cause of the variable CDG clinical features is not yet understood. Indeed, PMM2-CDG (and other CDG types) clinical manifestations vary among affected individuals, ranging from a severe antenatal presentation with multisystem involvement to mild adulthood presentation that is limited to minor neurological involvement. Previous attempts to prove a correlation between *PMM2* mutations and clinical phenotype (Altassan et al. 2019; Martínez-Monseny et al. 2019) have failed. To identify differentially regulated molecules and pathways in CDG cells, we decided to use Epstein-Barr virus (EBV)-transformed CDG B-LCL cells as a cellular model due to several advantages: (a) EBV-transformed CDG B-LCL cells are easily established in vitro (Bergmann et al. 1998; Orvisky et al. 2003) and represent a continuous and stable source of CDG cells (Çalışkan et al. 2014); (b) transformed B-LCL cells are secretory cells that are forced to proliferate and continuously synthesize proteins, such as immunoglobulins, cytokines or other cell-to-cell communication molecules, so their ER is chronically stressed and (c) as immune system cells, they express common genes and share common regulatory mechanisms with nervous system cells, such as neurons, which are affected cells in most CDG patients. Moreover, CDG patients often are affected by severe dysfunction of their humoral immune system (Lyons et al. 2015; Monticelli et al. 2016) in which B lymphocytes play the pivotal role.

In this work, we generated a collection of 13 EBV-transformed PMM2-CDG B-LCL cell lines derived from 13 different unrelated PMM2-CDG patients and performed transcriptome computational

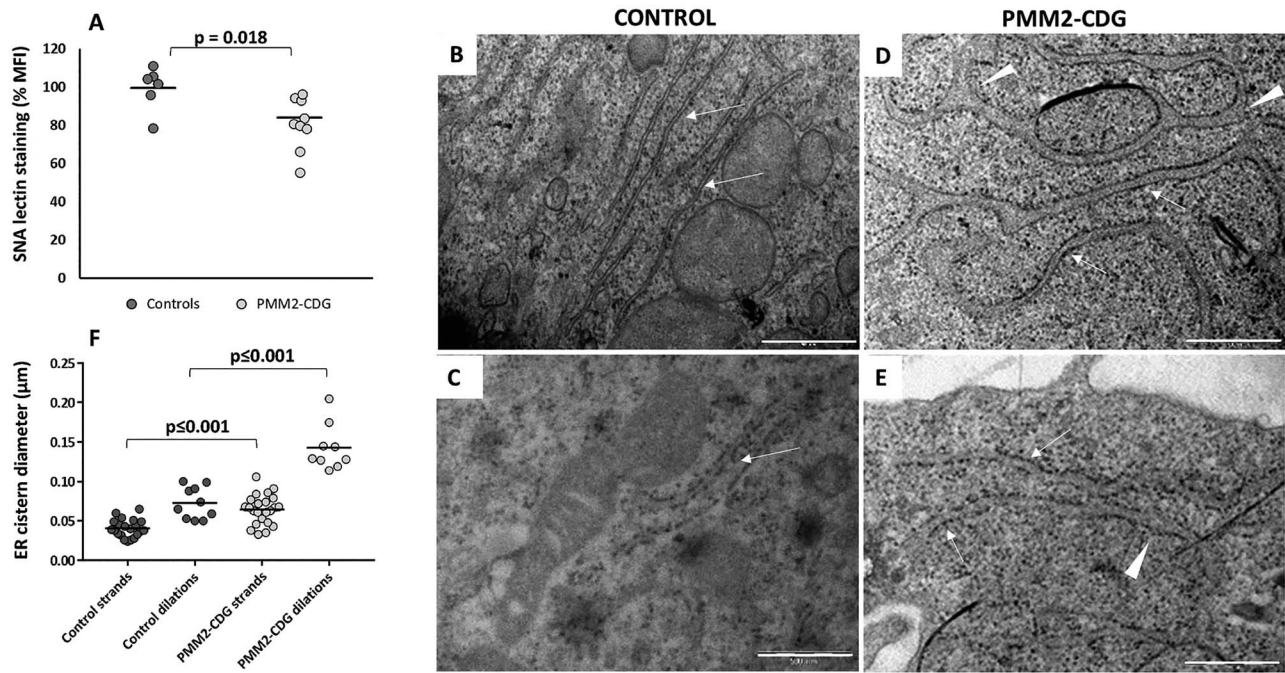


**Fig. 1.** Hyposialylation and ER structure of PMM2-CDG LCL-B lymphocytes. **(A)** SNA lectin was used to detect surface expression of  $\alpha$ 2,6-linked sialic acid. Nine PMM2-CDG (LCL-1, -2, -3, -10, -11, -12, -13, -16 and -17) and six (GUS, WEWAK, DMAR, TRAL, LG-15 and R69) control LCLs were harvested and incubated with biotin conjugated SNA lectin solution and PE-Cy7 conjugated streptavidin and analyzed by flow cytometry. Values (mean of three to seven determinations) are expressed as % MFI versus that observed in control cell lines. **(B–E)** Rough ER ultrastructure in PMM2-CDG (LCL-10, **D**, and LCL-12, **E**) and control LCL-B lymphocytes (DMAR, **B**, and WEWAK, **C**). **(F)** Distribution of diameters of both strands (arrows) and expanded (triangles) ER cisterns. Each dot represents the mean value of one cell. Horizontal black lines represent the mean value in each group of data. Transmission electron microscopy reveals notable dilated ER cisterns in PMM2-CDG LCL. White bars = 0.5  $\mu$ m.

and proteomic analysis with the aim to identify gene signatures in this cellular model that could potentially hint to dysfunctional biological pathways in PMM2-CDG versus healthy cells. Our data revealed a group of 490 dysregulated genes in severe B-LCL CDG cells, and 24 of them were also associated to the development and function of the nervous system that could represent potential CDG biomarkers, given these patient's clinical phenotypes. Besides, the expression of gene sets related to the UPR, the ER, GA, ribonucleic acid (RNA) metabolism and mitochondria function were affected and the dysregulation of carbonic anhydrase 2 (CA2) and ADAM23 (Disintegrin And Metalloproteinase Domain-Containing Protein 23) genes was confirmed. Our results support PMM2-CDG EBV-transformed B-LCL as a suitable cell model that expands both our knowledge and tools to study CDG pathology at the cellular level and could also be used to test the functional characteristic and potential therapeutic drugs for CDG.

## Results

### Hyposialylation, ER stress signs and cellular hypoglycosylation markers in PMM2-CDG Epstein-Barr virus transformed B cell lines

Three CDG-LCL were previously shown to express less  $\alpha$ 2,6 sialylated glycans in comparison to other cell lines (Bergmann et al. 1998). First, we expanded this study by determining the *Sambucus nigra* agglutinin (SNA) lectin staining of nine EBV-transformed B CDG versus six control LCL. Our results showed a significant lower SNA staining on CDG-LCL supporting the reduced surface expression of  $\alpha$ 2,6 sialylated glycans. CDG LCL-1 and LCL-13, two cell lines

generated from patients with severe clinical phenotype, showed the lowest levels of  $\alpha$ 2,6 sialylation (Figure 1A). Additionally, we examined the CDG-LCL ER structures in exponentially growing cells via transmission electron microscopy aiming to find new clues of ER stress, which is induced when abnormal N-glycosylation occurs (Oslowski and Urano 2011). Thus, the diameter of both strands and enlarged rough ER cisterns was measured in PMM2-CDG LCL-10 and LCL-12, cell lines also generated from patients with severe clinical phenotype, and in DMAR and WEWAK control LCL. As shown in Figure 1B–F, results indicated a significant caliber increase of rough ER cisterns in PMM2-CDG ( $64 \pm 19$  nm and  $143 \pm 30$  nm for strands and expanded ER cisterns, respectively) compared to the control LCL ( $41 \pm 11$  nm and  $73 \pm 20$  nm) of both ER strands and dilation areas. We next evaluated the ICAM-1 and LAMP1 expressions (using flow cytometry and western blot techniques, respectively), two common cellular glycosylation markers shown previously to be diminished in CDG fibroblast and amniocytes (He et al. 2012; Morelle et al. 2017; Radenkovic et al. 2019; Ferrer et al. 2020). We found that the expression of both proteins was decreased (35.1% and 46.5% mean reduction of ICAM-1 and LAMP1, respectively) in many of our cell lines derived from patients with different clinical severity as compared to control cells (Figure 2A–D). Finally, we tested PMM2 expression by western blot in three PMM2-derived LCL cells (LCL-10, -11 and -12) and three control cell lines (GUS, WEWAK and R69). This analysis revealed a heterogeneous but decreased expression of PMM2 in PMM2-CDG derived LCL cells (Figure 2E).

Altogether, these results indicated features of reduced PMM2 expression, hypoglycosylation and ER stress in our PMM2-CDG cell lines. Consistent with these observations, EBV-transformed B cell

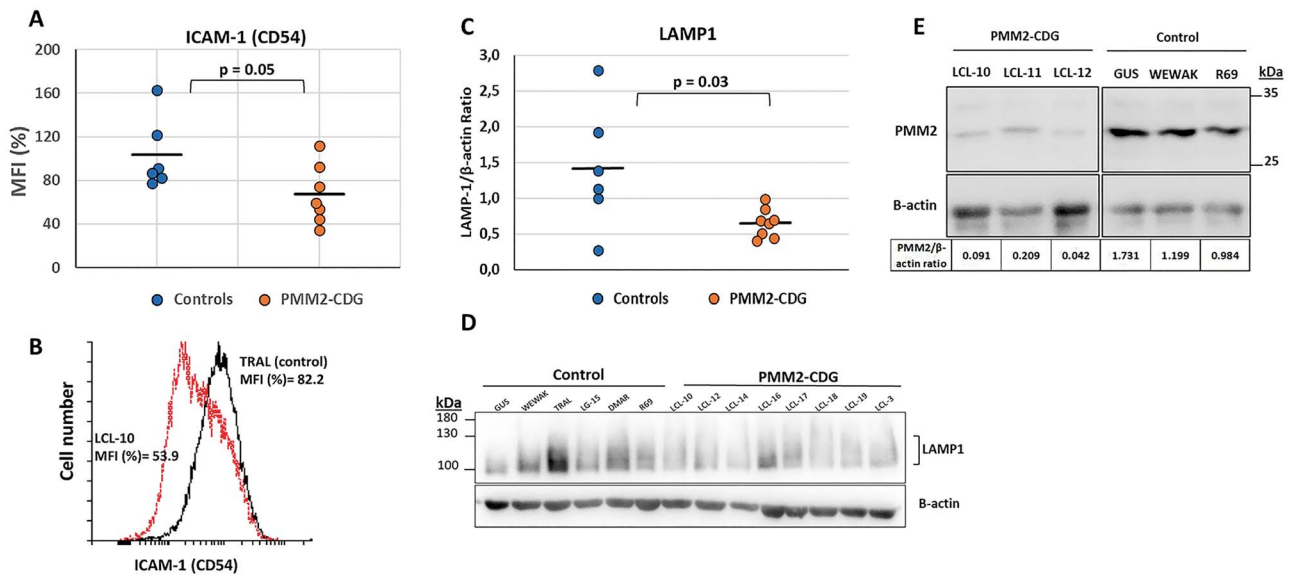


**Fig. 2.** Protein hypoglycosylation markers ICAM-1 (CD54) and LAMP1 and PMM2 protein were down-regulated in PMM2-CDG LCL. **(A, B)** ICAM-1 surface expression was determined by flow cytometry on LCL-2, -3, -10 to -13, and -18 PMM2-CDG versus GUS, WEWAK, TRAL, DMAR, LG15 and R69 control LCL **(A)**. A representative PMM2-CDG (LCL-10) versus control LCL (TRAL) cytometry histogram is shown in **(B)**. LAMP1 expression **(C, D)** was determined by western blot in LCL-3, -10, -12, -14, -16 to -19 PMM2-CDG versus GUS, WEWAK, TRAL, DMAR, LG15 and R69 control LCL. Horizontal bars in the figures represents mean values in each group. **(E)** PMM2 protein expression in LCL-10, -11, -12 versus GUS, WEWAK and R69 control LCL. The numbers below the bands indicate the corresponding expression levels relative to  $\beta$ -actin.

lines were chosen as a model to search for specific differences of gene expression associated with CDG condition.

### Differentially expressed genes and validation of gene array data by quantitative reverse transcriptase-polymerase chain reaction

Gene expression profile was assessed by using RNA microarray analysis on seven CDG cell lines generated from seven PMM2-CDG patients bearing different severe pathogenic mutations, serum transferrin hypoglycosylation and clinical neurological manifestations and from seven healthy cell lines (LCL-1, -2, -3, -10 to -13; [Table I](#) and [Materials and methods](#) section). We first analyzed data from protein-coding genes according to Student's  $t$  test and  $P < 0.05$ . Considering values of fold change (FC)  $\geq 2.5$ , we found 348 up-regulated genes and 106 down-regulated genes within all PMM2-CDG cell lines tested, as shown in [Figure 3A](#) and [Supplementary Tables I](#) and [II](#). Differential expression patterns of the top 25 up- or down-regulated genes between these two different conditions is shown by clustered heatmapping in [Figure 3B](#).

To verify the data from microarray analysis, the expression of eight up-regulated and three down-regulated genes of interest were examined by quantitative reverse transcriptase-polymerase chain reaction (QRT-PCR). Selection was based on their expression level, FC and cellular and/or tissue function as follows: (a) a direct role on the glycosylation pathway (*MAN1A1*, *MGAT2* and *B3GALT4*); (b) regulation of ER response to stress (*TXNDC5*, *PDIA4* and *P4HB*) and (c) genes that, according to reported CDG clinical symptoms, may be related to CDG pathology, such as ion channel genes (*KCNA3* and *CLIC6*) ([Izquierdo-Serra et al. 2018](#)), those involved in both the development and maintenance of the nervous system and/or activation and response of immune cells (*ADAM23*, ([Elizondo et al. 2016](#); [Hsia et al. 2019](#)) or involved on extracellular

matrix organization and regulation of cell proliferation such as *P3H2* ([Pokidysheva et al. 2014](#)) ([Table II](#)). More interesting, *CA2* gene, implicated in intracellular pH regulation, and showing a 6.37-fold increased expression in PMM2-CDG cells, was chosen because, recently, it has been shown a good relationship between patient-reported symptoms and treatment ([Martínez-Monseny et al. 2019](#)). PMM2-CDG and control samples evaluated by QRT-PCR included the original ones used in the arrays and four PMM2-CDG (LCL-14–LCL-17) ([Table I](#)) and two additional control B LCL lines (KCAR and JY). As shown in [Figure 4](#), the relative expression levels of all tested genes exhibited the same regulatory trend without exception as compared with the microarray analysis. These results validated the data obtained by microarray analysis and suggest new 11 potential biomarkers that describe the PMM2-CDG condition.

### Gene expression analysis

The above sets of over- and underexpressed genes were investigated using Molecular Signatures Database (MSigDB) collections, which compute overlaps between our gene sets (up-regulated and down-regulated genes described above) and gene sets in MSigDB. Differentially expressed genes mainly implicated components of the cell membrane, ER and GA. Analysis showed that genes significantly increased in PMM2-CDG cells overlapped to gene sets/families of genes such as transcription factors (54 genes), regulators of cell differentiation (56 genes), response to stress (39 genes), cytokine production (31 genes), the apoptotic process (50 genes), adhesion (40 genes), motility and cell junction (43 genes), whereas decreased genes significantly overlapped to synapse (18 genes), signaling pathways (14 genes) and some of them to cell junction gene sets (14 genes) ([Supplementary Table III](#)). Interestingly, further analysis of those up- and down-regulated genes showing abundant expression on the arrays (50 up-regulated and 18 down-regulated genes) indicated significant overlapping with concepts, such as regulation of nervous

**Table I.** Demographic, genetic, biochemical and clinical data of PMM2-CDG patients from which EBV-transformed B lymphoblastoid cell lines (B-LCLs) were obtained

B-LCL	Gender	PMM2 mutations	Carbohydrate-deficient serum transferrin (%) <sup>a</sup>	Antitrombin activity (%)	FXI activity (%)	Nervous system involvement <sup>c</sup> (no. of items = 6 max.)
LCL-1 <sup>b</sup>	F	p.R141H/p.V231M	ND	ND	ND	6
LCL-2 <sup>b</sup>	F	p.R141H/p.D188G	ND	ND	ND	6 <sup>d</sup>
LCL-3 <sup>b</sup>	F	p.R141H/p.D188G	ND	ND	ND	6 <sup>d</sup>
LCL-10 <sup>b</sup>	M	p.E33X/p.V44A	61.38	17	27.3	6
LCL-11 <sup>b</sup>	M	p.R141H/p.Y64C	59.85	46	59.4	6
LCL-12 <sup>b</sup>	F	p.P113L/p.F207S	25.74	9	24.5	6
LCL-13 <sup>b</sup>	F	p.P113L/p.T118S + P184D	67.63	22	19.3	4
LCL-14	F	p.F157S/p.R162W	25.83	63	92.4	4
LCL-15	M	p.L32R/p.F207S	23.98	72	ND	2
LCL-16	F	p.L32R/p.F157S	50.46	69	ND	2
LCL-17	F	p.R123Q/p.C241S	80.20	100	90	2
LCL-18	M	p.G214S/p.G214S	78.56	106.2	124.7	3
LCL-19	M	p.R141H/p.C241S	79.50	100.4	117.4	3
Pooled normal serum	—	—	7.89 ± 0.78	100%	100%	—

ND, not determined; FXI, plasma coagulation factor XI. <sup>a</sup>Percentage of total asialo-, disialo- and trisialotransferrin. <sup>b</sup>PMM2-CDG LCL tested in arrays. <sup>c</sup>Items are: Ataxia HP:0001251; Cerebellar atrophy HP:0001272; Peripheral neuropathy HP:0009830; Stroke-like episodes HP:0002401; Epilepsy HP:0001250; Intellectual disability HP:0001249. <sup>d</sup>Exitus, severe clinical phenotype according to Mattheijs et al. (2000).

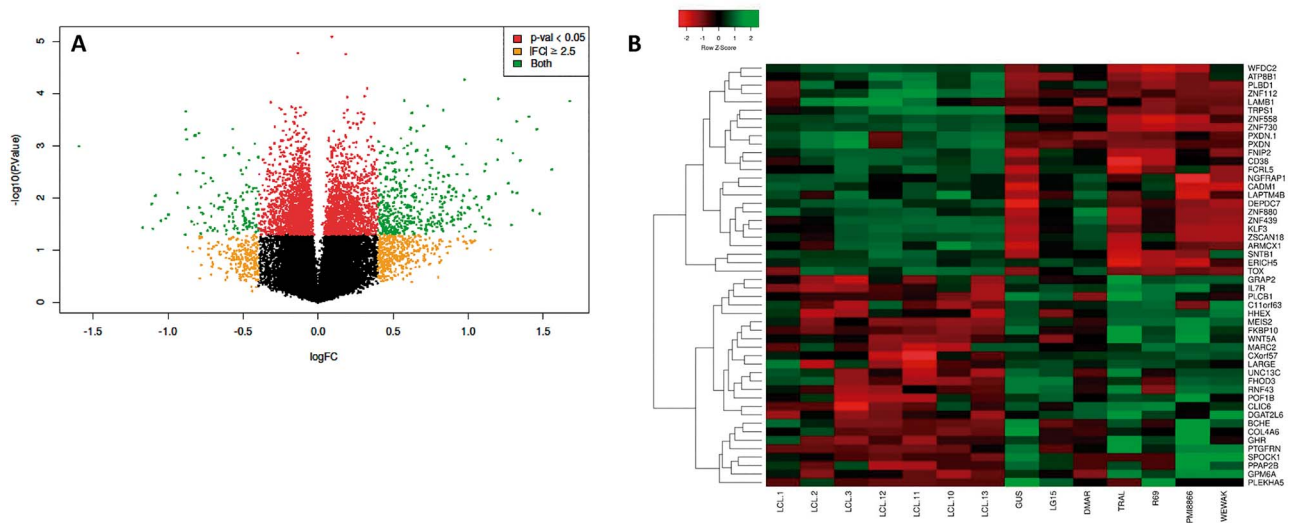


**Fig. 3.** Transcriptome profile of PMM2-CDG LCL-B lymphocytes. **(A)** Volcano plot showing differentially expressed genes in PMM2-CDG cells with  $P$ -value < 0.05 and  $FC \geq 2.5$  (green dots). LogFC versus  $-\log_{10} P$ -value is represented. **(B)** Heat map of the hierarchical clustering of the top 25 commonly regulated genes depicting their expression patterns and variation in CDG (LCL-1, -2, -3 and LCL-10, -11, -12 and -13) or control cell lines. The color key indicates the direction of changes, with green depicting genes significantly up-regulated ( $P$ -value < 0.05 and FC ranging between 47.35 and 12.28 values) and red showing genes significantly down-regulated ( $P$ -value < 0.05 and FC ranging between -39.21 and -5.68). Genes were clustered based on their expression values across samples using complete linkage function and the Euclidean distance measurement method.

system development and cell (neuron) differentiation, regulation of lysosome organization, synapsis and cell projection. As shown in Table III, the overlapped genes were the overexpressed *SCARB2*, *SOCS2*, *RAPGEF2*, *ZC4H2*, *SEMA4D*, *NAP1L2*, *MECP2*, *GF11*, *PRKACB*, *NEDD9*, *TGFB11I*, *CA2*, *CD109*, *LAMB1*, *NEFH* and *LAPTM4B*. The overlapped underexpressed genes were *UNC13C*, *ABHD17C*, *CPEB1*, *WASF1*, *SYBU*, *AUTS2*, *ITGB3*, *WWC1*, and *ADAM23*. Among them, we can underline those genes known to be expressed in a broad range of human tissues, including immune and nervous system cells, reported to affect development and function, such as: *SEMA4D* (FC = 2.84), a member of the semaphorin family of neural guidance proteins, expressed in embryonic and adult

brain, immune cells and platelets, which promotes the migration of cerebellar granule cells (reviewed by Wannemacher et al. 2011); *CA2* (FC = 6.37), with a role in neuronal signaling (Imtaiyaz Hassan et al. 2013); *AUTS2* (FC = -3.10), role in brain development and behavior in animal models and role in neuronal migration, Hori and Hoshino 2017); *UNC13C* (FC = -5.05), specific developmental mediator at the glutamatergic synapse in cerebellar cortex (Kusch et al. 2018); and *ADAM23* (as defined in Table II). All together, these genes exemplify the first reported group of differentiated genes associated with CDG condition in PMM2-CDG cells, which could represent additional potential cellular biomarkers for CDG pathology involving both the immune and nervous systems.

**Table II.** Up-regulated and down-regulated genes used for array validation; array statistic data and cellular characteristics of the encoded protein are shown

Gene	Protein	PMM2-CDG versus control		Location and cellular functions
		P-value	FC	
CA2	Carbonic anhydrase II	0.028	6.37	Intracellular pH regulation. Expression possibly related to patient-reported symptoms and treatment (Martínez-Monseny et al. 2019)
MAN1A1	Alpha-1,2-mannosidase IA	0.002	4.16	GA. Protein glycosylation metabolic pathway
MGAT2	Mannosyl (alpha-1,6-)-glycoprotein beta-1,2-N-acetylglucosaminyltransferase	0.000	1.53	
B3GALT4	Beta-1,3-galactosyltransferase 4	0.047	2.96	GA. Glycosphingolipid biosynthesis
TXNDC5	Disulfide isomerase protein ERp46	0.001	2.67	ER and GA. Facilitates the formation of disulfide bonds and correct folding of nascent polypeptides. Increased expression in ER stress response
PDIA4	Protein disulfide-isomerase A4 (ERp72)	0.000	2.03	
P4HB	Prolyl 4-hydroxylase (beta subunit, PDI family)	0.001	1.61	Plasma and intracellular membranes. Regulation of ion transport. Involved in the central nervous system and hematopoietic cell function
KCNA3	Voltage-gated potassium channel (Kv1.3)	0.012	4.75	
CLIC6	Chloride intracellular channel 6	0.004	-8.34	Plasma membrane. Important role in cell-to-cell interaction. Involved in the development and maintenance of the nervous system and in the activation and response of immune system
ADAM23	Disintegrin and metalloproteinase domain-containing protein 23 (MDC3)	0.017	-4.36	
P3H2	Prolyl 3-hydroxylase 2 (LEPREL1)	0.015	-6.97	ER, GA, sarcoplasmic reticulum. Collagen metabolic process. Extracellular matrix organization Negative regulation of cell proliferation

Besides *MAN1A1*, *MGAT2* and *B3GALT4* genes (Table II), we found five additional up-regulated and two down-regulated genes implicated in the glycoprotein/proteoglycan biosynthetic process. Those genes encoded for four sulfotransferases (*CHST15* [FC = 6.09]; *HS3ST1* [FC = 5.28]; *CHST12* [FC = 3.88]; *CHST4* [FC = -2.87]), two glycosyltransferases (*ST8SIA5* [FC = 3.20]; *LARGE* [FC = -5.68]) and one galactosidase (*GLB1L3*; FC = 6.09), as shown in Supplementary Tables I and II. These results suggest changes on complex N-glycan maturation, biosynthesis and remodeling of proteoglycan, glycosphingolipid,  $\alpha$ -dystroglycan and O-glycosyl compounds in the CDG condition. Gene expression responsible for GPI-anchor biosynthetic process were not affected (not shown).

### Computed functional analysis

To further identify biological consequences due to gene expression changes on PMM2-CDG cells, we used gene set enrichment analysis (GSEA), which generated predictions for significantly increased or decreased biological concepts related to gene ontology (GO) terms. The GSEA descriptive statistics, Normalized Enrichment Score (NES), Nominal P-value  $\leq 0.05$  and false discovery rate (FDR)  $q$ -value  $\leq 0.25$ , were used to discriminate significance. First, we looked for alteration on cellular processes that were described previously (Lecca et al. 2005) to be expected for CDG condition, such as increased expression of ER stress response genes due to unfolded protein accumulation. As expected, and consistent with the observed dilated ER morphology (Figure 1), GSEA revealed significant positive enrichment for concepts, including ER UPR, regulation of response to ER stress and UPR, regulation of retrograde protein transport from ER to cytosol and regulation of ERAD pathway in B-LCL from PMM2-CDG patients (Figure 5). Moreover, UPR stress sensor IRE1, ATF6 and PERK pathways were also

up-regulated, although only IRE1 pathway (involved in genes activation conducted to increase the ER protein-folding capacity and to decrease protein load entering the ER, Sicari et al. 2019) was statistically significant. FC increase of UPR-implicated genes ranged between 1.34 and 2.95 (P-value < 0.05). Those values were comparable to those obtained by Lecca and collaborators in CDG type I fibroblasts (Lecca et al. 2005). Our results suggest that CDG condition in our cell lines is associated with an ER stress state that is mainly controlled by IRE1 pathway genes and characterized by the up-regulation of genes involved in the ERAD pathway to increase the removal of polypeptides that fail to reach their native state.

Further analysis on GO biological processes identified new gene sets modulated by the CDG condition. As shown in Figure 6, gene sets related to inosine monophosphate (IMP) biosynthetic process, genesis of mitochondrion and ribosomes were significantly underexpressed, whereas gene sets related to transport of vesicles between ER and GA as well as GA organization were significantly overexpressed on PMM2-CDG cells. Accordingly, analysis regarding GO cellular components showed that genes associated with all different GA compartments and vesicles, including both COPI and COPII transport vesicle components, were significantly overexpressed in PMM2-CDG cells (Figure 7). In the ER, gene expression of components involved in quality control (*CALR*, *EDEM-1*, -2, -3, *ERLEC1*), chaperones (*HSP90B1*, *P4HB*, *PDIA6*, *PDIA4* and *TXNDC5*) and the oligosaccharyltransferase (OST) complex were also up-regulated (Supplementary Table IV and data not shown). Up-regulation of important gene encoding components involved in ERAD substrates ubiquitination, such as *SYVN1* (FC = 2.04) and *RNF103* (FC = 3.06), were also detected (not shown). Furthermore, defined transcripts for components of protein complexes that function in protein translocation across the ER were more abundant in CDG cells. Lysosomal lumen components were also up-regulated (Figure 6). These results suggest an augmented control of the nascent proteins biogenesis entering the

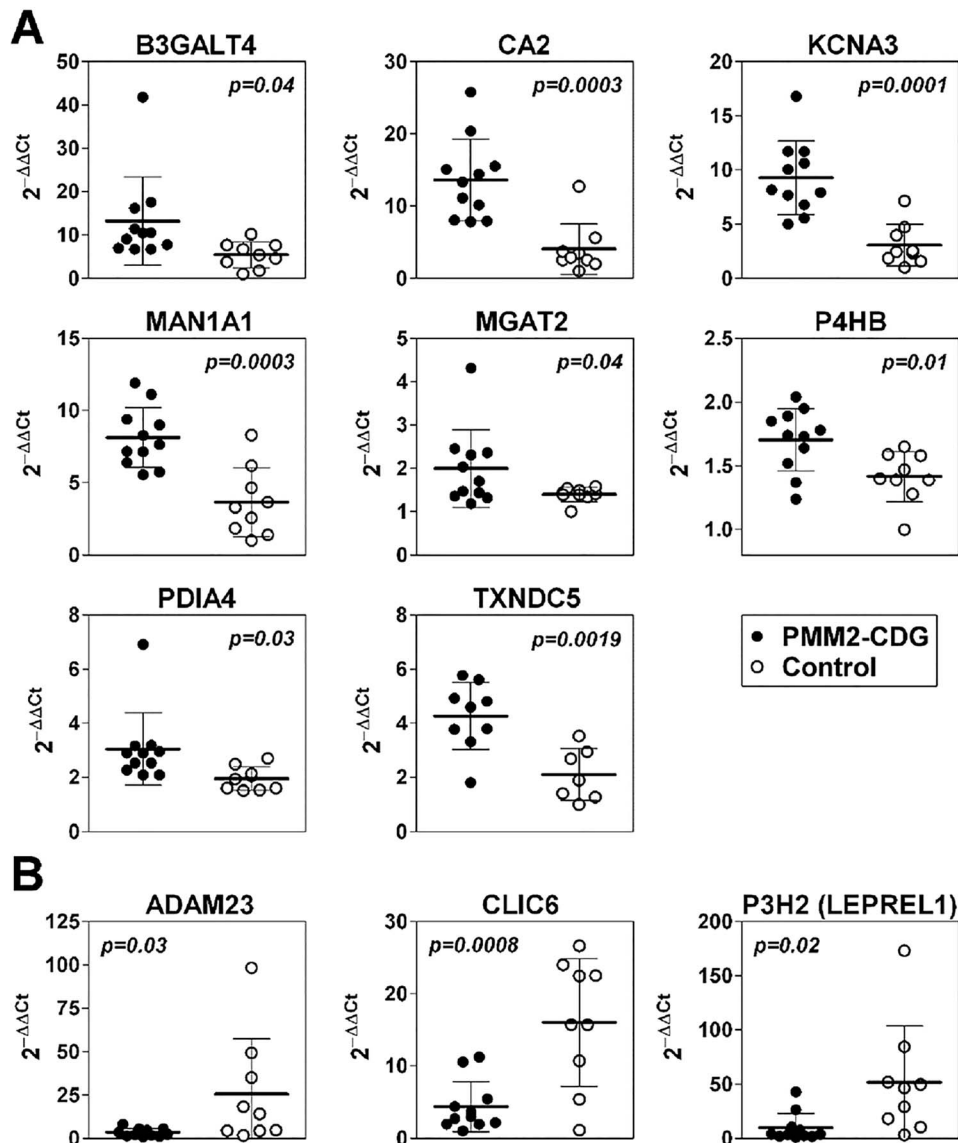


**Fig. 4.** Validation of PMM2-CDG versus control gene expression. QRT-PCR values are depicted for eight up-regulated (A) and three down-regulated (B) genes found in the RNA array analysis. QRT-PCR included a total of 11 PMM2-CDG and nine control B LCL cells that were the original ones used in the arrays and four additional PMM2-CDGs (LCL-14, -15, -16 and -17) (Table I) and two 2 control B LCL lines (KCAR and JY).

secretory pathway and an intensification of the secretory pathway in CDG cells by increasing cellular component dedicated to both anterograde and retrograde traffic of vesicles between ER and GA in PMM2-CDG cells.

Gene sets related to glycosylation/de-glycosylation pathways in the ER and GA such as GO MANNOSIDASE ACTIVITY, GO ACETYLGALACTOSAMINYLTRANSFERASE ACTIVITY, GO CHONDROITIN SULFOTRANSFERASE ACTIVITY or GO CHONDROITIN SULFATE BIOSYNTHETIC PROCESS, reached a NOM  $P$ -value  $\leq 0.05$  and the highest NES scores, although an FDR  $q$ -value  $\leq 0.25$ , indicating not significant enrichment (Supplementary Figure 1) despite the dysregulated mannosidases, sulfotransferases and glycotransferases expression data named above. These results indicated the lack of an important glycosylation/deglycosylation pathway dysregulation in our group of PMM2-CDG cell lines. Apoptosis-related gene sets were not significantly enriched (not

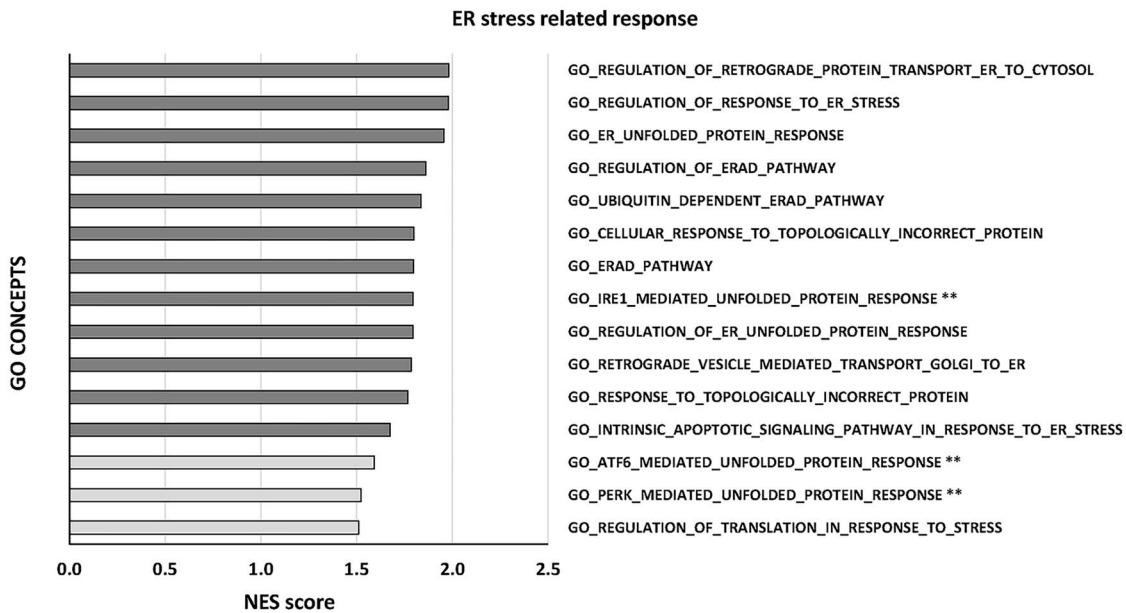
shown), although some individual apoptosis related genes were up-regulated as mentioned above.

Down-regulated gene sets related to cellular components affected mitochondria, ribosomes and RNA metabolic components of the CDG cells (Table IV). Regarding the mitochondria (Table IV, panel A), GSEA analysis revealed a significant reduced expression of genome gene encoding proteins localized in the outer and inner membrane complexes, the mitochondrial matrix and nucleoid. The highest NES scores were reached for cytochrome complex, respiratory complex IV and TIM23 mitochondrial inner membrane protein translocase complex gene sets. Genes involved in the expression of the mitochondrial contact site and cristae organizing system (MICOS) complex were also underexpressed.

Regarding ribosomes, gene encoding both cytoplasmic and mitochondrial ribosome component were underexpressed in CDG cells as well as the translation initiation factor 2b complex (Table IV, panel

**Table III.** Computed overlaps between 50 up-regulated and 18 down-regulated abundant genes expressed by PMM2-CDG B LCL cells and GO gene sets in MSigDB

Gene set name		# Genes in gene Set	# Genes in overlap	P-value	FDR q-value	Genes in overlap
UP-regulated	GO_REGULATION_OF_NERVOUS_SYSTEM_DEVELOPMENT	914	9	2.65E-6	1.08E-2	SCARB2, SOCS2, RAPGEF2, ZC4H2, SEMA4D, NAP1L2, MECP2, GFI1, PRKACB
	GO_REGULATION_OF_CELL_DIFFERENTIATION	1863	12	3.92E-6	1.08E-2	SCARB2, SOCS2, RAPGEF2, ZC4H2, SEMA4D, NAP1L2, MECP2, GFI1, NEDD9, TGFB11, CA2, CD109
	GO_NEURON_DIFFERENTIATION	1348	10	8.49E-6	1.08E-2	SCARB2, SOCS2, RAPGEF2, ZC4H2, SEMA4D, NAP1L2, MECP2, GFI1, LAMB1, NEFH
	GO_REGULATION_OF_LYSOSOME_ORGANIZATION	5	2	1.69E-5	1.72E-2	SCARB2, LAPTM4B
Down-regulated	GO_CELL_PROJECTION_PART	1440	8	1.29E-7	1.28E-3	UNC13C, ABHD17C, CPEB1, WASF1, SYBU, AUTS2, ITGB3, WWC1
	GO_NEURON_PART	1715	7	7.65E-6	3.04E-2	UNC13C, ABHD17C, CPEB1, WASF1, SYBU, AUTS2, ADAM23
	GO_SYNAPSE	1171	6	1.13E-5	3.04E-2	UNC13C, ABHD17C, CPEB1, WASF1, ITGB3, AUTS2, ADAM23

**Fig. 5.** ER stress response processes modulated by differentially expressed genes in PMM2-CDG cells. NES derived from the GSEA using the GO BIOLOGICAL PROCESSES gene sets. Positive NES values suggest an up-regulation of the respective set. Only those gene sets displayed in red are significantly enriched with an adjusted NOM  $P$ -value  $\leq 0.05$  and FDR  $q$ -value  $\leq 0.25$ . \*\*UPR stress sensor pathways.

B). Regarding RNA metabolic process, both cytoplasmic and nuclear components were down-regulated, including RNA polymerases I and II, spliceosome and exosome, the cytoplasmic methylosome and survival motor neuron (SMN) complexes (Table IV, panel

C), indicating a reduction of transcription, processing of most RNA types (ribosomal RNA, messenger RNA [mRNA], snRNA and microRNAs) and translation of mRNAs, which reduces protein synthesis and avoids the ER collapse (Sicari et al. 2019).

## GO - Biological processes

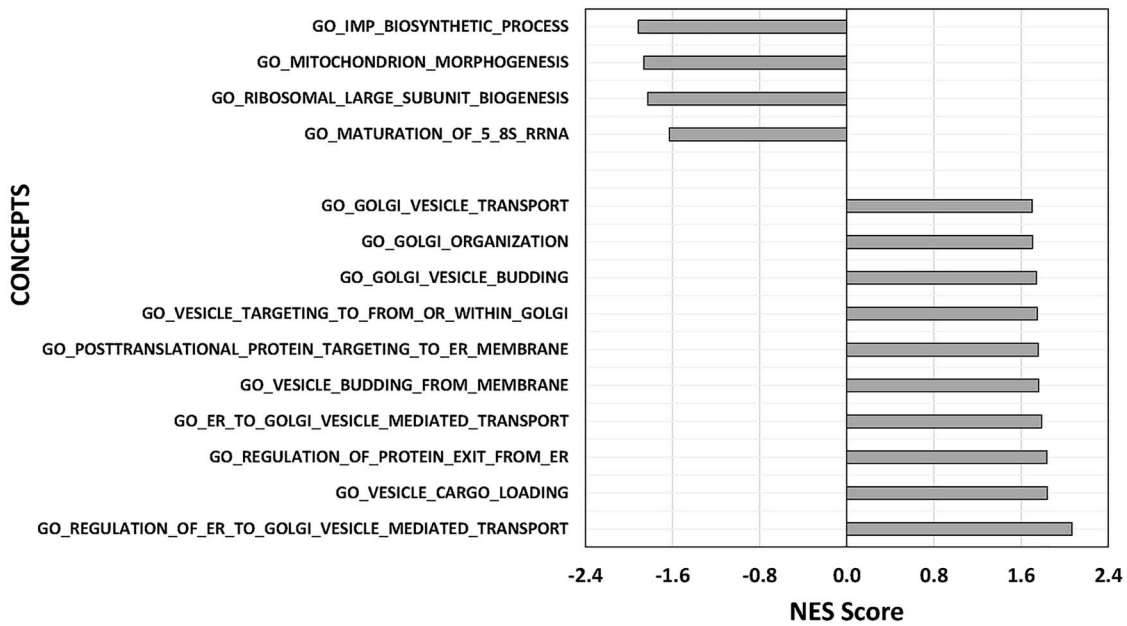


**Fig. 6.** NES derived from the GSEA using the GO Biological Processes gene sets. Positive NES values suggest an up-regulation and negative NES suggest a down-regulation of their respective sets. Only gene sets displaying significant enrichment (adjusted NOM  $P$ -value  $\leq 0.05$  and FDR  $q$ -value  $\leq 0.25$ ) are represented.

## Positively Enriched GO-Cellular Components

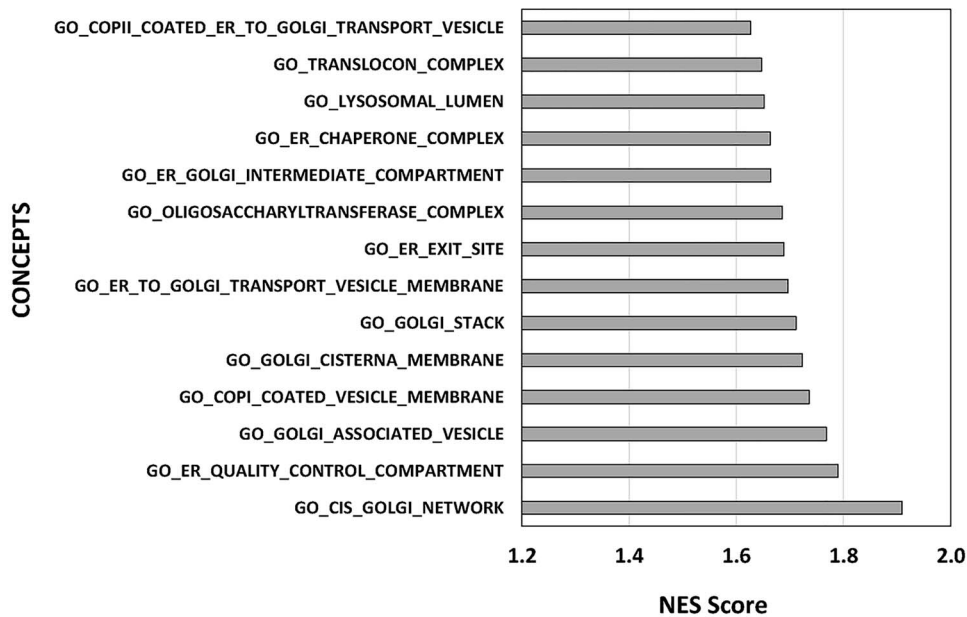


**Fig. 7.** Positive enriched gene sets in PMM2-CDG cells derived from GSEA using the GO cellular component gene sets. NES (positive values) of gene sets displaying significant enrichment (NOM  $P$ -value  $\leq 0.05$  and FDR  $q$ -value  $\leq 0.25$ ) are represented.

Among these genes, we can emphasize the important genes *SMN1* (FC = -1.36, essential component of the SMN complex, associated with the neurodegenerative disorder spinal muscular atrophy, Lefebvre et al. 1995), the RNA exosome components *EXOSC2* (FC = -1.46) and *EXOSC3* (FC = -1.27) (whose mutations cause a syndrome with various tissue-specific phenotypes, including retinitis

pigmentosa and mild intellectual disability and pontocerebellar hypoplasia type 1b, respectively (Morton et al. 2018) and, related to the mitochondria, *DNAJC19* (FC = -1.47; motor component of the TIM23 mitochondrial import inner membrane translocase complex) and *TACO1* (FC = -1.27, translational activator of mitochondrial encoded cytochrome c oxidase I) (data not shown).

**Table IV.** Down-regulated gene sets related to cellular components of mitochondrion (A), ribosomes (B) and molecular complexes involved in RNA metabolic processes (C) in PMM2-CDG cells; ES and NES derived from the GSEA using the GO gene sets; only statistically significant gene sets (adjusted NOM *P*-value  $\leq 0.05$  and FDR *q*-value  $\leq 0.25$ ) are shown; negative ES values suggest a down-regulation of the respective set; general concepts are represented in bold

(A) CONCEPT (mitochondrion)	GENESET SIZE	ES	NES	NOM <i>P</i> -value	FDR <i>q</i> -value
GO_OUTER_MITOCHONDRIAL_	16	-0.66085	-1.62287	0.017	0.173
MEMBRANE_PROTEIN_COMPLEX					
GO_INNER_MITOCHONDRIAL_	97	-0.54374	-1.73243	0.004	0.084
MEMBRANE_PROTEIN_COMPLEX					
GO_INTRINSIC_COMPONENT_OF_	40	-0.56775	-1.67967	0.012	0.131
MITOCHONDRIAL_INNER_MEMBRANE					
GO_EXTRINSIC_COMPONENT_OF_	11	-0.72821	-1.66323	0.014	0.143
MITOCHONDRIAL_INNER_MEMBRANE					
GO_TIM23_MITOCHONDRIAL_IMPORT_	14	-0.78104	-1.83611	0.000	0.080
INNER_MEMBRANE_TRANSLOCASE_					
COMPLEX					
GO_CYTOCHROME_COMPLEX	25	-0.63349	-1.75372	0.000	0.088
GO_RESPIRATORY_CHAIN_COMPLEX_IV	15	-0.63480	-1.62206	0.018	0.164
GO_MICOS_COMPLEX	7	-0.80921	-1.56582	0.021	0.218
GO_MITOCHONDRIAL_MATRIX	440	-0.49335	-1.82209	0.000	0.066
GO_NUCLEOID	40	-0.66560	-1.77194	0.004	0.087
<b>(B) CONCEPT (ribosome)</b>	<b>GENESET</b>	<b>ES</b>	<b>NES</b>	<b>NOM</b>	<b>FDR</b>
	<b>SIZE</b>			<b><i>P</i>-value</b>	<b><i>q</i>-value</b>
GO_RIBOSOME	222	-0.52904	-1.77501	0.002	0.092
GO_SMALL_RIBOSOMAL_SUBUNIT	69	-0.56387	-1.74158	0.002	0.085
GO_LARGE_RIBOSOMAL_SUBUNIT	115	-0.59399	-1.80535	0.002	0.065
GO_ORGANELLAR_RIBOSOME	86	-0.64658	-1.74449	0.012	0.088
GO_ORGANELLAR_SMALL_RIBOSOMAL_	28	-0.73255	-1.75270	0.002	0.083
SUBUNIT					
GO_ORGANELLAR_LARGE_RIBOSOMAL_	56	-0.62348	-1.61052	0.050	0.178
SUBUNIT					
GO_PRERIBOSOME	69	-0.70247	-1.70808	0.004	0.100
GO_PRERIBOSOME_LARGE_SUBUNIT_	22	-0.71312	-1.61820	0.042	0.167
PRECURSOR					
GO_EUKARYOTIC_TRANSLATION_	6	-0.87851	-1.83083	0.002	0.070
INITIATION_FACTOR_2B_COMPLEX					
<b>(C) CONCEPT (RNA metabolic process)</b>	<b>GENESET</b>	<b>ES</b>	<b>NES</b>	<b>NOM</b>	<b>FDR</b>
	<b>SIZE</b>			<b><i>P</i>-value</b>	<b><i>q</i>-value</b>
GO_RNA_POLYMERASE_COMPLEX	103	-0.50107	-1.67403	0.006	0.136
GO_RNA_POLYMERASE_I_COMPLEX	12	-0.74370	-1.54614	0.010	0.231
GO_RNA_POLYMERASE_II_HOLOENZYME	77	-0.45047	-1.58419	0.011	0.208
GO_SMALL_NUCLEOLAR_RIBONUCL	26	-0.66800	-1.53272	0.063	0.247
EOPROTEIN_COMPLEX					
GO_U1_SNRNP	20	-0.56446	-1.55414	0.050	0.230
GO_U4_SNRNP	10	-0.72992	-1.58489	0.029	0.212
GO_U6_SNRNP	8	-0.74489	-1.65513	0.008	0.146
GO_U7_SNRNP	7	-0.78391	-1.57344	0.023	0.216
GO_SMALL_SUBUNIT_PROCESSOME	33	-0.73574	-1.64763	0.012	0.153
GO_PRECATALYTIC_SPLICEOSOME	43	-0.52589	-1.55332	0.059	0.228
GO_SMN_COMPLEX	12	-0.72504	-1.57340	0.022	0.212
GO_SMN_SM_PROTEIN_COMPLEX	17	-0.74068	-1.64752	0.008	0.148
GO_METHYLOSOME	12	-0.78023	-1.66042	0.004	0.142
GO_EXOSOME_RNASE_COMPLEX_	25	-0.55711	-1.62216	0.016	0.169
GO_CYTOPLASMIC_EXOSOME_RNASE_COMPLEX_	14	-0.77823	-1.84618	0.002	0.130
GO_NUCLEAR_EXOSOME_RNASE_COMPLEX_	16	-0.73793	-1.84914	0.000	0.243

Additionally, some gene encoding components of the dendritic spine membrane gene set were significantly down-regulated (NES = -1.6386; NOM *P*-value = 0.022; FDR *q*-value = 0.1589; not shown), such as *DDN* (FC = -1.62, gene encoding

dendrin, a protein of unknown function that accumulates in dendritic spines (Neuner-Jehle et al. 1996; Herb et al. 1997) and *SHISA8/CKAMP39* (FC = -2.18), encoding an auxiliary protein subunit that regulates AMPAR proteins, glutamate receptors

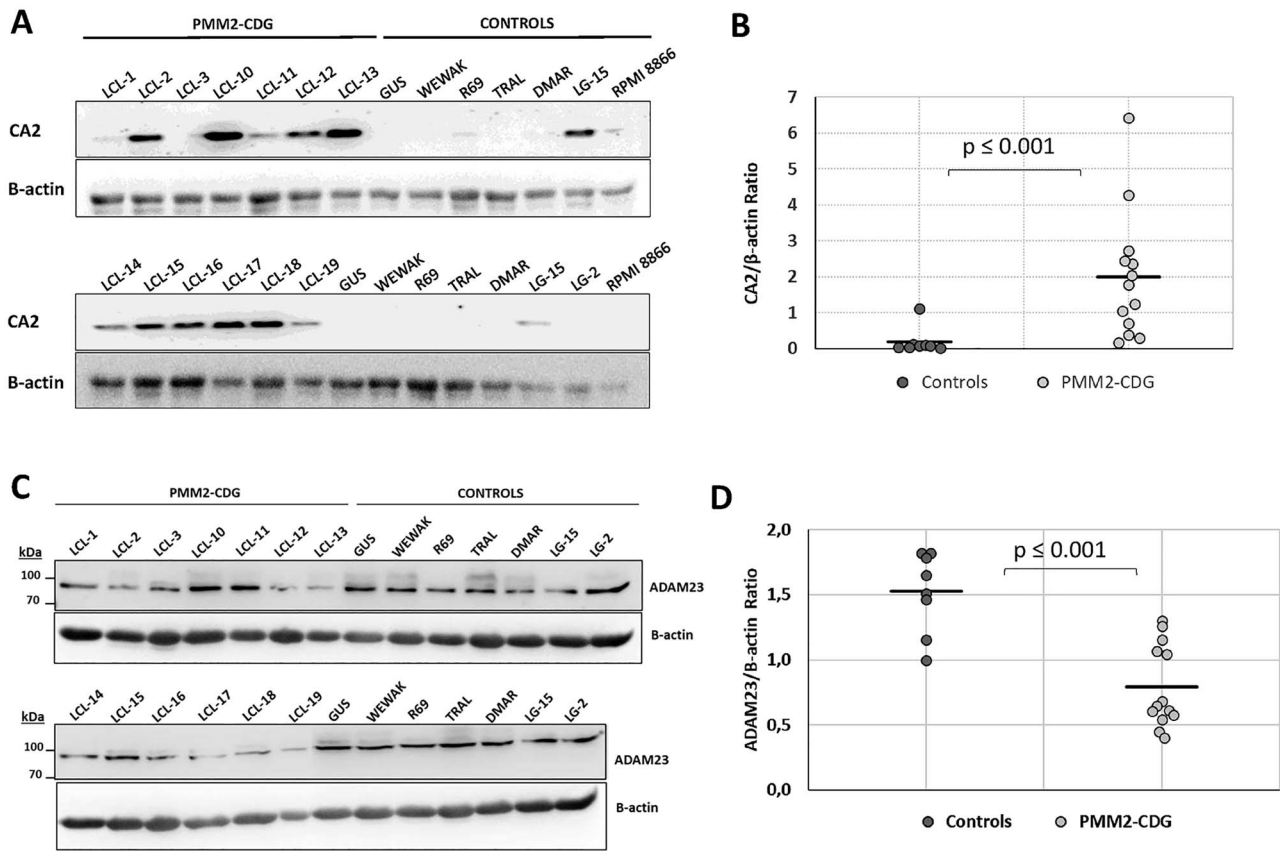


**Fig. 8.** CA2 and ADAM23 protein expressions in PMM2-CDG and control LCL. Cellular extracts from the indicated LCL were analyzed by western blotting to test total CA2 and ADAM23 proteins. (A, C) Figures depict representative blots out of three with similar results. (B, D) Figures represent protein/b-actin ratio mean values from all three determinations. Horizontal black lines represent the mean value in each group of data.

of fast excitatory transmission in the central nervous system (Farrow et al. 2015).

### Protein expression of CA2 and ADAM23 potential markers

Finally, to observe the impact of some transcriptional changes on protein expression, we further studied the expression of CA2 and ADAM23 by western blot. PMM2-CDG and control LCL included in this analysis were those evaluated by the QRT-PCR (LCL-1, -2, -3, -10, -11, -12, -13, -14, -15, -16 and -17) and two additional PMM2-CDG (LCL-18 and -19) (Table I). In agreement with microarrays and QRT-PCR data, we found a significant increase of CA2 (Figure 8A and B) and a decrease of ADAM23 (7C and 7D) protein expression in our PMM2-CDG group of cell lines compared to control LCL. PMM2-CDG LCL-10 and LCL-13 showed the highest levels of CA2 protein, whereas LCL-2, -12 and -13 showed the lowest levels of ADAM23 protein among cells lines derived from patients with severe clinical phenotype. A high level of CA2 was not significantly associated with a low level of ADAM23 protein. Additionally, hypoglycosylation bands were not identified in ADAM23 blots despite its eight potential N-glycosylation sites and the use of a polyclonal anti-ADAM23 antibody. Other heavily glycosylated proteins were tested by western blot as well, such as CD58 (six potential N-glycosylation sites), SEMA4D (six potential N- and six O-glycosylation sites) and  $\beta$ 1-integrin (*ITGB1*, CD29; 12 potential N-glycosylation sites). As for LAMP1, no hypoglycosylated forms of

all these proteins were detected (Supplementary Figure 2). Altogether, protein expression values showed a similar trend with arrays FC values. Correlation between protein and gene expression, including both PMM2-CDG and control cells, were statistically significant for ADAM23 and SEMA4D (Supplementary Table V).

### Discussion

The present work yields insights into the dysregulated genes affected in PMM2-CDG cells by means of RNA microarray analysis, which was validated by both QRT-PCR and protein expression. Our results demonstrate PMM2-CDG B LCL cells as a novel and accurate cellular model in the CDG field and confirm CA2 protein as a valuable PMM2-CDG biomarker.

EBV-transformed B LCL cells have been used previously as a cellular model of different human diseases. They have been considered surrogate cells in neurological disorder studies (Sie et al. 2009). As an example, LCLs have been utilized to identify candidate genes and cellular functions for autism spectrum disorders (ASDs) (Hu et al. 2009; Frye et al. 2017) and as drug response prediction model for pharmacogenomics research in cancer and immunosuppression, including drug response differences according to individual genetic variation (Çalışkan et al. 2014; Jack et al. 2014). In the case of CDG, some LCLs were generated in the past to study the glycosylation differences between LCLs of healthy persons and CDG-patients (Bergmann et al. 1998), PMM activity (Orvisky et al. 2003), to

determine a *PMM2* genetic variant (Tayebi et al. 2002) and to study some cellular metabolic defects of three GDP-mannose pyrophosphorylase A-CDG-affected siblings (Koehler et al. 2013). To the best of our knowledge, B-LCLs have not been further used.

Regarding protein glycosylation defects, we found a decreased surface  $\alpha$ 2,6 sialylated glycans, ICAM-1, LAMP1 and *PMM2* expression in *PMM2*-CDG B-LCL. Detection of hypoglycosylated protein isoforms or glycan site-occupancy defects are the strongest evidence of hypoglycosylation in type I CDG. Indeed, differential protein glycoforms have been detected in CDG patient's plasma (Wopereis et al. 2005; Bruneel et al. 2017; de la Morena-Barrio et al. 2019; López-Gálvez et al. 2020) besides transferrin glycoforms, which is the gold-standard plasma CDG biomarker. Low ICAM-1 and LAMP2 expressions have been considered to be hypoglycosylation cellular markers for CDG fibroblast or amniocytes (He et al. 2012; Ferrer et al. 2020), although hypoglycosylated isoforms were not detected. However, glycoforms have been mainly detected in secreted rather than cellular CDG proteins. Thus, our results confirmed the differences that CDG may cause at the levels of cellular proteins, although we were not able to detect the presence of hypoglycosylated forms of five potential heavily glycosylated cellular proteins, such as LAMP1, ADAM23, SEMA4D, CD58 and  $\beta$ 1-integrin. This fact may be explained by different hypothesis: (a) analytical techniques, such as western blot, might not reach enough sensitivity to detect low levels of hypoglycosylated forms; (b) antibodies used in this study might poorly recognize hypoglycosylated forms and (c) hypoglycosylated forms of cellular proteins could be degraded. Nevertheless, a *PMM2* protein decrease was also observed in spite that no differences with control cells were detected at mRNA (arrays) level. Altogether, our results reveal LCL as an advantageous cellular model that helps to expand both our knowledge and tools to study CDG pathology at the cellular level. Further studies are required to find additional hypoglycosylation cellular markers in CDG.

Using GSEA analysis, we proved if UPR network was up-regulated in *PMM2*-CDG cells and studied the level of this increase. We found significant up-regulation of gene sets related to ER stress-sensor IRE1 pathway, UPR regulation and ERAD pathway, including retrograde protein transport to cytosol in *PMM2*-CDG LCL lines (Figure 5), with the absence of enriched expression of the ER stress-induced apoptotic pathway. The related FC values obtained, ranging between 1.34 and 2.95 ( $P$ -value < 0.05), were somewhat higher than those found on CDG type I fibroblasts by Lecca et al. (2005), although they were much lower to those obtained in tunicamycin-treated fibroblasts reported by the same authors. Opposite to tunicamycin-treated normal cells, our data indicate a physiological UPR with the absence of apoptotic features in *PMM2*-CDG LCL cells. Thus, *PMM2*-CDG LCLs reveal an adaptive moderate UPR that could enable the use of these cells as a model for examination of CDG ER stress under different experimental conditions, including drug response for therapeutic drug testing.

Acute accumulation of unfolded proteins due to hypoglycosylation in the ER activates coordinated UPR signaling pathways to reduce protein synthesis by means of mRNA degradation and translation attenuation. However, little is known about how the UPR relates to post-ER events in GA and mitochondria compartments and even how ER newly synthesized proteins are exported from the ER to other cellular compartments during a prolonged UPR (Sicari et al. 2019). Knowledge about adaptive chronic UPR, and its impact on CDG condition, is even more limited. Our data extend our understanding and suggest that CDG UPR may be maintained by a continuous decreased level of transcription of RNA encoding ribosomal (both cytoplasmic and mitochondrial), spliceosome, exosome and

methylosome components. These results suggest that adaptive chronic UPR maintains an attenuation of transcription, RNA maturation and translation to maintain a low rate of protein synthesis and possible modifications in the RNA splicing process. GA and mitochondria stress events that are induced by accumulation of unfolded proteins in the ER or in the GA itself have also been poorly studied and, again, knowledge is limited to experiments that use pharmacological glycosylation inhibition on normal cellular models. In this sense, our data showed that RNA encoding mitochondrial respiratory chain components are decreased in *PMM2*-CDG cells as well, revealing an interconnection between organelles (ER-mitochondria-GA) to maintain cellular proteostasis during a chronic UPR (Sasaki and Yoshida 2015; Sicari et al. 2019). Reduction or deficiencies in the level of specific function and components, such as RNA processing, energy production and protein synthesis, may have harmful consequences in many organs and systems.

Transcription factor XBP1, the major regulator of the UPR, induces the expression of several gene encoding enzymes, such as *MAN1A1* and *MGAT2* (Dewal et al. 2015), indicating that the UPR may regulate *N*-glycan biosynthetic process as well. Our results are in line with and expand these observations since new dysregulated glyco-genes have been detected. Gene sets related to demannosylation, heparan sulfate and chondroitin sulfate biosynthetic processes were not significantly enriched; however, specific transcripts involved in glycosylation processes, such as GA mannosidase *MAN1A1* and several sulfotransferases and glycotransferases, were strongly over- or underexpressed, which suggests that mutations in *PMM2* may also alter ganglioside biosynthesis and *N*-glycan and glycosaminoglycan maturation by dysregulation of specific genes, such as *B3GALT4*, *MAN1A1*, *MGAT2*, *ST8SIA5*, *LARGE*, *GLB1L3*, *CHST15*, *HS3ST1*, *CHST12* and *CHST4*. Among them, reduced expression of *LARGE* and *CHST4* could be of importance since reduced activity of *LARGE* gene may cause congenital muscular dystrophy and mental retardation (Longman et al. 2003), while changes in *CHST4* expression may be associated to glycan-mediated cell adhesion and trafficking (Veerman et al. 2019).

GSEA analysis identified a significant down-regulation of genes dedicated to IMP biosynthetic process (Figure 6). This finding is interesting since cellular IMP levels could regulate mannosidase activity of *PMM1*, a paralogous enzyme of *PMM2*, whose activity does not compensate for *PMM2* deficiency in *PMM2*-CDG patients. Elevated IMP levels stimulated *PMM1* hexose biphosphate phosphatase activity but inhibited its mutase activity (Veiga-da-Cunha et al. 2008; Citro et al. 2017). These, together with our observation, suggest that a decrease in IMP synthesis would increase the residual *PMM* activity in *PMM2*-CDG cells. However, in these conditions, IMP biosynthesis would depend more on the purine salvage pathway, which consumes inosine. Since inosine may be particularly relevant for neuronal axon growth (Chen et al. 2002; Kim et al. 2013), these metabolic interpretations suggest novel therapeutic interventions.

Correlation between biochemical and clinical CDG phenotypes is still a difficult task. Clinical severity of *PMM2*-CDG has been explained only in part by the partial loss of *PMM2* activity, but several other features remain under hypothetical consideration, including specific additional gene mutations (Bortot et al. 2013), patient's genetic background and epigenetic contribution. Recently, partially deficient or variant genes present in the general population have been found, which could be associated and act as modifiers of *PMM2* activity (Citro et al. 2018). Our data bring into focus a new hypothesis in which the dysregulation of group of genes (in B lymphocytes and other cell types), due to the chronic UPR condition and driven by different dysregulated transcription factors, could be related and

explain, at least in part, clinical CDG phenotypes. Among these genes, we have paid attention to those both expressed by LCL cells and involved in glycosylation (*MAN1A1*, *MGAT2*, *CHST4* and *LARGE*) and the nervous system development and function (the cerebellum in particular), such as *ADAM23*, *SEMA4D*, *UNC13C*, *AUTS2*, *CA2*, *SMN1*, *EXOSC2*, *DDN* and *SHISA8*. Among them, *ADAM23*, and specially *CA2*, have been shown here to be dysregulated. Our data indicate further considerations such as the level of specific genes expression in each individual patient not only as mRNA but also at the protein level and, more intricate, the unbalanced expression among these specific genes in the absence of other pathologic mutations. Situations that require the production of a large amount of proteins could contribute to the CDG pathogenesis. Reduction or deficiencies in the level of RNA processing and energy production may have additional harmful consequences. Since individual genetic variations are conserved following EBV transformation (Çalışkan et al. 2014), these aspects deserve further research on CDG-LCL cells. Due to the involvement of *CA2* in the pathophysiology of PMM2-CDG patients (Martínez-Monseny et al. 2019), our results confirm the importance of *CA2* protein as unique cellular biomarker and therapeutic target for PMM2-CDG.

## Materials and methods

### Patients, sample collection and analysis of PMM2 genetic variants and abnormal protein glycoforms

Eligible patients were between 2 and 20 years of age and had molecularly confirmed PMM2-CDG. Demographic, biochemical and clinical characteristics of the population (using HPO–Human Phenotype Ontology codes) are detailed in Table I.

Peripheral blood samples from PMM2-CDG patients were collected into citrate tubes and delivered within 24 h from the hospitals of reference Sant Joan de Deu (Barcelona) and Hospital Universitario Virgen de la Arrixaca (Murcia) to the IMIB laboratories in Murcia, Spain, at room temperature, where all further studies were done. Blood samples were drawn during noninfectious periods of patients. Controls, patients and relatives were fully informed of the aim of this study, which was performed according to the declaration of Helsinki, as amended in Edinburgh in 2000. Written informed parental consents were obtained since all enrolled CDG patients were children. This study obtained approval from the University of Murcia Ethics Committee.

PMM2 variant analysis of LCL-1, -2 and -3 cell lines was performed by molecular analysis of all eight exons and flanking regions of the *PMM2* gene as previously described (Matthijs et al. 1998). Due to the genetic variants that these LCLs were holding, their clinical phenotypes were assigned as severe (Table I), according to Matthijs et al. 2000. Abnormal glycoforms of serum transferrin were evaluated by HPLC as previously described (Quintana et al. 2009) and were compared to a pooled normal serum. Antithrombin activity was determined using a chromogenic method, and the presence of abnormal glycoforms in plasma was evaluated by western blot essentially as reported (de la Morena-Barrío et al. 2012). FXI levels and hypoglycosylation was evaluated by a coagulometric assay and western blot as described elsewhere (de la Morena-Barrío et al. 2019).

### Generation and culture of CDG EBV-transformed B cell lines

Three EBV-transformed CDG B-LCL cell lines (LCL-1, LCL-2 and LCL-3) were established previously as described (Bergmann et al.

1998). New established CDG B cell lines (LCL-10–LCL-19) were obtained from different PMM2-CDG patients (Table I) by using purified PBMC that were cultured with supernatants from Cotton-top Tamarin Monkey EBV-leukocyte cell line B95-8 (kindly provided by Dr. Martí, CIBERER Biobank, Valencia, Spain) as previously described (Miller and Lipman 1973). LCLs were non-monoclonal and were confirmed by testing for a variety of B cell antigens by flow cytometry (Bergmann et al. 1998). PMM2-CDG B-LCL-10 to -19 have not been reported before.

Control B-LCL cell lines used were GUS (Hernandez-Caselles et al. 1993), LG15 (Aparicio et al. 1987), DMAR (generated for this study), TRAL and KCAR (Martí et al. 1983), R69 (Perussia et al. 1987), WEWAK (Rooney et al. 1984), RPMI 8866 (ECACC 95041316) and JY (ECACC 94022533).

Both CDG and control cell lines were grown as suspension cultures in Iscove's modified Dulbecco's culture medium supplemented with 10% fetal calf serum, 1% glutamine, 1% antibiotics (penicillin and streptomycin) (Biowest, France). Newly established LCL lines were cultured at least for 2 months before harvesting for RNA extraction or any other determination. Cells growing at exponential phase for several days were pelleted and preserved in RNAlater solution until RNA isolation.

### Flow cytometry experiments

SNA lectin staining was performed by using SNA (Vector Labs, CA, USA) conjugated to biotin which recognized  $\alpha$ 2,6-linked sialic acid. Exponentially growing LCL ( $10^5$  cells) were washed twice with phosphate buffered saline (PBS) and were incubated with the lectin solution (20  $\mu$ g/mL in PBS) for 10 min at room temperature. Then cells were resuspended in PBS supplemented with BSA 0.2%, washed again and incubated with streptavidin conjugated to PE-Cy7 fluorochrome for 10 min. After removing the excess of streptavidin, stained cells (10,000) were collected using a FACS Canto cytometer (Becton-Dickinson, Mountain View, CA, USA).

For ICAM-1 staining, an APC conjugated anti-ICAM-1 antibody from Biolegend (clone HCD54; San Diego, CA, USA) was used following manufacturer's instructions.

Data were further analyzed using the CellQuest program (Becton Dickinson) and Flowing Software version 2.5.1 to obtain the mean fluorescence intensity (MFI) and the percentage of SNA and ICAM-1 staining as described (García-López et al. 2016).

### Transmission electron microscopy

Exponentially growing LCLs were harvested and washed with PBS. Cells were fixed with 2.5% glutaraldehyde in 0.1 M sodium cacodylate buffer for 15 min and were then post-fixed in potassium ferrocyanide-reduced osmium tetroxide 1% for 30 min, dehydrated in ethanol gradient and gradually embedded in Epon 812 resin. Ultrathin sections (Leica EM10C ultramicrotome) were mounted onto formvar carbon-coated copper grids and contrasted with uranyl acetate and lead citrate. Ultrastructure was examined using a Philip Tecnai 12 transmission electron microscope supplied with a Megaview G3 camera at 80 kV. Ten to 12 cells from two control and two PMM2-CDG LCL were randomly examined. Diameter of both strands and expanded areas of ER cisterns were determined by using *ImageJ* software (<https://imagej.nih.gov/ij/>).

### RNA isolation and microarray analysis

Seven PMM2-CDG LCL (LCL-1, -2, -3, -10, -11, -12 and -13) from patients bearing pathologic genetic variants, strong

serum protein hypoglycosylation and severe clinical neurological manifestations were tested (Table 1) against seven (GUS, WEWAK, LG-15, TRAL, DMAR, R69 and RPMI8866) control LCLs. Cells in RNAlater were pelleted and total RNA was isolated by using RNeasy Mini Kit (Qiagen, Germantown, MD, USA) following manufacturer's instructions. Isolated RNA was quantified in a Nanodrop spectrophotometer and RNA quality was analyzed in an Agilent 2100 Bioanalyzer. RNA Integrity Number of samples was  $9.6 \pm 0.8$  (mean  $\pm$  SD), with values  $>7.0$  for all samples. A pooled sample composed of equimolar amounts of RNA from four control B-LCL cells and four control NK cells was used as reference.

For microarray analysis, reference and test RNA samples were labeled using Agilent Two Color (cyanine-3-CTP [Cy3] and cyanine-5-CTP [Cy5], respectively) Quick Amp Labeling and RNA Spike-In kits (Agilent, Santa Clara, CA, USA), according to the manufacturer's protocol. Microarray experiments were designated as *PMM2-CDG* ( $N = 7$ ) or *CTRL* ( $N = 7$ ) and were performed using SurePrint G3 Human Gene Expression v3 Microarray Kit targeting 26083 Entrez genes and 30606 lncRNA transcripts. *PMM2* probe sequence was mapped at the *PMM2* gene 3'-untranslated region, indicating that patient's mutations are not included in these arrays.

The labeled chromosomal RNAs were mixed and hybridized onto the microarray slides using the Agilent Gene Expression Hybridization kit. After hybridization, the microarray slides were washed and scanned in an Agilent G2565CA DNA Microarray Scanner. Datasets, expressed as  $\log_{10}$  ratios for test versus reference, were computed from images by the Agilent Feature Extraction software by using normalization by linear and Lowess methods. Dataset series were deposited at the Gene Expression Omnibus database under accession number *GSE145082*. Datasets were transformed into  $\log_2$  ratios. Comparison between values from *PMM2-CDG* and *CTRL* experiments was performed using the Student *t*-test and *P*-values, which were computed using Excel software. Mean values from different conditions were subtracted (*PMM2-CDG* - *CTRL*) and FCs were calculated using the formulas  $2^{(PMM2-CDG - CTRL)}$  for positive changes and  $-2^{-(PMM2-CDG - CTRL)}$  for negative changes. Differentially expressed genes were chosen if  $FC \geq 2.5$  (overexpressed),  $FC \leq -2.5$  (underexpressed) and *P*-value  $< 0.05$ .

### QRT-PCR

Array data were validated by QRT-PCR of 11 (eight up-regulated and three down-regulated) mRNAs in 11 *PMM2-CDG* cells and nine *CTRL* cells. RNA samples were subjected to reverse transcription with the iScript cDNA Synthesis Kit (Bio-Rad), following the manufacturer's instructions. QRT-PCR was performed with the SYBR Premix Ex Taq (Takara Bio, Mountain View, CA) in an ABI Prism 7000 Sequence Detection System (Applied Biosystems, Foster City, CA). Predesigned SYBR green primers H\_B3GALT4\_1, H\_CA2\_1, H\_KCNA3\_1, H\_MAN1A1\_1, H\_MGAT2\_1, H\_P4HB\_1, H\_PDIA4\_1, H\_TXNDC5\_2, H\_ADAM23\_1, H\_CLIC6\_1 and H\_LEPREL1\_1 (P3H2) were used and, as a reference for normalization, QuantiTect primer assay for GAPDH (cat. no. QT01192646, Qiagen). The relative expression values, expressed as FC relative to the reference, were calculated using the formula  $2^{-\Delta Ct}$  as described elsewhere (Ruiz-Lafuente et al. 2014). Differences between *PMM2-CDG* and *CTRL* were considered significant when the *P*-value  $< 0.05$  according to the Student's *t*-test.

### GSEA

We explored gene set size differences and analyzed correlations between our dataset analysis and the *a priori* defined set of genes included in the MSigDB database v7.0 (<http://software.broadinstitute.org/gsea/>) (Subramanian et al. 2005; Liberzon et al. 2015). GSEA was used to find overrepresentations of gene sets subjected to GO C5 terms (GO biological process, GO cellular components and GO molecular function; 9996 gene sets) in *PMM2-CDG* versus control cells by using the complete array data. Analysis was run under 1000 phenotype type of permutations, weighted enrichment statistic and signal2noise metric for ranking genes. GSEA analysis provided an enrichment score (ES), that reflects the degree to which a set is overrepresented at the extremes (top or bottom) of the entire ranked list of genes in the array, and a normalized ES score (NES) for each gene set to account for the size of the set. A nominal (NOM) *P*-value  $< 0.05$  and FDR  $< 0.25$  of the enriched gene sets were considered to be statistically significant.

### Western blot analysis of protein expression

Exponentially growing LCL cells were harvested, washed twice with PBS, pelleted, lysed (lysis buffer composed by Tris buffer 50 mM pH 7.4, 150 mM NaCl, 1% Nonidet P-40, 1 mM PMSF and 1% Protease Inhibitor Cocktail [P8340 from Merck Life Science]) and were analyzed by western blot under reduced conditions as described (Hernández-Caselles et al. 2019). Western blot primary antibodies were rabbit polyclonal antihuman ADAM23, from Invitrogen (Carlsbad, CA, USA), and mouse monoclonal antihuman CA2, mouse monoclonal antihuman *PMM2*, mouse monoclonal antihuman SEMA4D (CD100), mouse monoclonal anti-LAMP1 (clone H4A3) and anti- $\beta$ -actin from Santa Cruz Biotechnology (Heidelberg, Germany). Antihuman CD58 (clone TS2/9) and antihuman  $\beta$ 1-integrin (clone TS2/16) monoclonal antibodies were from hybridoma culture supernatants, kindly provided by Dr. Sanchez-Madrid (Hospital Universitario de la Princesa, Madrid, Spain). Immunoblots were detected by using the Enhanced Chemiluminescence System<sup>®</sup> (Amersham ECL<sup>™</sup> Prime Western Blotting Detection Reagent, GE Healthcare, United Kingdom). Protein bands were quantified by densitometry using ImageJ software and expressed as relative to  $\beta$ -actin total protein.

### Statistical analysis

Results were reported as mean  $\pm$  SD and represented as bar graphs as specified in the figures. Mann-Whitney *U* test was used for analysis of sialylation levels, ER cistern diameter and protein expression. Significance was assigned to a *P*-value  $\leq 0.05$  in all cases. Analysis was performed using IBM SPSS Statistics 21.0 software (IBM Corporation, NY).

### Supplementary data

Supplementary data are available at *Glycobiology* online.

### Authors' contributions

G.R., T.H.-C., A.E.-S., R.S.-A. and L.A. performed B cell transformation and cell culture. A.P., N.R.-L. and T.H.-C. carried out RNA extraction, arrays and QPCR. M.E.D.I.M.-B. and J.C. carried out LCL's *PMM2* mutations and abnormal serum protein isoform studies. M.S. and S.I.-M. selected the patients and carried out the

clinical studies. T.H.-C. and G.R. performed electron microscopy studies. T.H.-C. carried out the GSEA statistical analysis, flow cytometry and western blot studies, designed the study and drafted the manuscript. All authors have read and agreed to the actual version of the manuscript.

## Acknowledgements

We would like to express our sincere gratitude to the patients and families who voluntarily participated in this study. We specially thank Dr. Rosa Moya-Quiles (Immunology Unit, Hospital Virgen de la Arrixaca, Murcia, Spain) for her generous support. We also thank María García-García (Microscopy Service, ACTI, University of Murcia) for her technical support and Dr. Fernando Pérez-Sanz (Biomedical Informatics & Bioinformatics Platform, IMIB) for his help in statistical analysis.

## Funding

This work was supported in part by the Fundación MEHUER (Medicamentos Huerfanos y Enfermedades Raras, Ayuda Santiago Grisolyá 2016), Sevilla (Spain) and the University of Murcia. Fundación MEHUER and University of Murcia were not involved in study design, in the collection, analysis and interpretation of data, in the writing of the report and in the decision to submit the article for publication. M.E.D.I.M.-B. is a holder of a post-doctoral research grant from the University of Murcia, Spain.

## Conflict of interest statement

None declared.

## Abbreviations

ADAM23, Disintegrin And Metalloproteinase Domain-Containing Protein 23; ASDs, autism spectrum disorders; CA2, carbonic anhydrase 2; CDG, congenital disorders of glycosylation; EBV, Epstein-Barr virus; ER, endoplasmic reticulum; ERAD, ER-associated degradation; ES, enrichment score; FDR, false discovery rate; GA, Golgi apparatus; GSEA, gene set enrichment analysis; GO, gene ontology; IMP, inosine monophosphate; iPSCs, induced pluripotent stem cells; LCL, lymphoblastoid B cell line; LLO, lipid-linked oligosaccharide; MFI, mean fluorescence intensity; MICOS, mitochondrial contact site and cristae organizing system; MSigDB, Molecular Signatures Database; NES, Normalized Enrichment Score; OST, oligosaccharyl-transferase; PBS, phosphate buffered saline; PDIs, protein disulfide isomerases; PMM2, phosphomannomutase 2; RNA, ribonucleic acid; SMN, survival motor neuron; UPR, unfolded protein response

## References

Altassan R, Péanne R, Jaeken J, Barone R, Bidet M, Borgel D, Brasil S, Cassiman D, Cechova A, Coman D, et al. 2019. International clinical guidelines for the management of phosphomannomutase 2-congenital disorders of glycosylation: Diagnosis, treatment and follow up. *J Inherit Metab Dis*. 42:5–28.

Aparicio P, Rojo S, Jaraquemada D, López de Castro JA. 1987. Fine specificity of HLA-B27 cellular allorecognition. HLA-B27f is a functional variant distinguishable by cytolytic T cell clones. *J Immunol*. 139:837–841.

Bergmann M, Gross HJ, Abdelaty F, Möller P, Jaeken J, Schwartz-Albiez R. 1998. Abnormal surface expression of sialoglycans on B lymphocyte cell

lines from patients with carbohydrate deficient glycoprotein syndrome I A (CDGS I A). *Glycobiology*. 8:963–972.

Bortot B, Cosentini D, Faletta F, Biffi S, De Martino E, Carrozzi M, Severini GM. 2013. PMM2-CDG: Phenotype and genotype in four affected family members. *Gene*. 531:506–509.

Bruneel A, Habarou F, Stojkovic T, Plouviez G, Bougas L, Guillemet F, Brient N, Henry D, Dupré T, Vuillaumier-Barrot S, et al. 2017. Two-dimensional electrophoresis highlights haptoglobin beta chain as an additional biomarker of congenital disorders of glycosylation. *Clin Chim Acta*. 470:70–74.

Çalışkan M, Pritchard JK, Ober C, Gilad Y. 2014. The effect of freeze-thaw cycles on gene expression levels in lymphoblastoid cell lines. *PLoS One*. 9:e107166. [10.1371/journal.pone.0107166](https://doi.org/10.1371/journal.pone.0107166).

Chan B, Clasquin M, Smolen GA, Histen G, Powe J, Chen Y, Lin Z, Lu C, Liu Y, Cang Y, et al. 2016. A mouse model of a human congenital disorder of glycosylation caused by loss of PMM2. *Hum Mol Genet*. 25:2182–2193.

Chen P, Goldberg DE, Kolb B, Lanser M, Benowitz LI. 2002. Inosine induces axonal rewiring and improves behavioral outcome after stroke. *Proc Natl Acad Sci U S A*. 99:9031–9036.

Citro V, Cimmaruta C, Liguori L, Viscido G, Cubellis MV, Andreotti G. 2017. A mutant of phosphomannomutase1 retains full enzymatic activity, but is not activated by IMP: Possible implications for the disease PMM2-CDG. *PLoS One*. 12:e0189629. [10.1371/journal.pone.0189629](https://doi.org/10.1371/journal.pone.0189629).

Citro V, Cimmaruta C, Monticelli M, Riccio G, Hay Mele B, Cubellis MV, Andreotti G. 2018. The analysis of variants in the general population reveals that PMM2 is extremely tolerant to missense mutations and that diagnosis of PMM2-CDG can benefit from the identification of modifiers. *Int J Mol Sci*. 19(8):2218–2229.

de la Morena-Barrio ME, Sevivas TS, Martinez-Martinez I, Miñano A, Vicente V, Jaeken J, Corral J. 2012. Congenital disorder of glycosylation (PMM2-CDG) in a patient with antithrombin deficiency and severe thrombophilia. *J Thromb Haemost*. 10:2625–2627.

de la Morena-Barrio ME, Wypasek E, Owczarek D, Miñano A, Vicente V, Corral J, Undas A. 2019. MPI-CDG with transient hypoglycosylation and antithrombin deficiency. *Haematologica*. 104:e79–e82.

Dewal MB, DiChiara AS, Antonopoulos A, Taylor RJ, Harmon CJ, Haslam SM, Dell A, Shoulders MD. 2015. XBP1s links the unfolded protein response to the molecular architecture of mature N-glycans. *Chem Biol*. 22:1301–1312.

Elizondo DM, Andargie TE, Marshall KM, Zariwala AM, Lipscomb MW. 2016. Dendritic cell expression of ADAM23 governs T cell proliferation and cytokine production through the  $\alpha(v)\beta(3)$  integrin receptor. *J Leukoc Biol*. 100:855–864.

Farrow P, Khodosevich K, Sapir Y, Schulmann A, Aslam M, Stern-Bach Y, Monyer H, von Engelhardt J. 2015. Auxiliary subunits of the CKAMP family differentially modulate AMPA receptor properties. *Elife*. 4:e09693. [10.7554/eLife.09693](https://doi.org/10.7554/eLife.09693).

Ferrer A, Starosta RT, Ranatunga W, Ungar D, Kozicz T, Klee E, Rust LM, Wick M, Morava E. 2020. Fetal glycosylation defect due to ALG3 and COG5 variants detected via amniocentesis: Complex glycosylation defect with embryonic lethal phenotype. *Mol Genet Metab*. 131:424–429.

Frye RE, Rose S, Wynne R, Bennuri SC, Blossom S, Gilbert KM, Heilbrun L, Palmer RF. 2017. Oxidative stress challenge uncovers trichloroacetaldehyde hydrate-induced mitoplasty in autistic and control lymphoblastoid cell lines. *Sci Rep*. 7:4478. [10.1038/s41598-017-04821-3](https://doi.org/10.1038/s41598-017-04821-3).

García-López R, de la Morena-Barrio ME, Alsina L, Pérez-Dueñas B, Jaeken J, Serrano M, Casado M, Hernández-Caselles T. 2016. Natural killer cell receptors and cytotoxic activity in phosphomannomutase 2 deficiency (PMM2-CDG). *PLoS One*. 11:e0158863. [10.1371/journal.pone.0158863](https://doi.org/10.1371/journal.pone.0158863).

He P, Ng BG, Losfeld M-E, Zhu W, Freeze HH. 2012. Identification of intercellular cell adhesion molecule 1 (ICAM-1) as a hypoglycosylation marker in congenital disorders of glycosylation cells. *J Biol Chem*. 287:18210–18217.

Herb A, Wisden W, Catania MV, Maréchal D, Dresse A, Seeburg PH. 1997. Prominent dendritic localization in forebrain neurons of a novel mRNA and its product, dendrin. *Mol Cell Neurosci*. 8:367–374.

- Hernández-Caselles T, Miguel RC-S, Ruiz-Alcaraz AJ, García-Peñarrubia P. 2019. CD33 (Siglec-3) inhibitory function: Role in the NKG2D/DAP10 activating pathway. *J Immunol Res.* 2019:6032141. [10.1155/2019/6032141](https://doi.org/10.1155/2019/6032141).
- Hernandez-Caselles T, Rubio G, Campanero MR, del Pozo MA, Muro M, Sanchez-Madrid F, Aparicio P. 1993. ICAM-3, the third LFA-1 counter-receptor, is a co-stimulatory molecule for both resting and activated T lymphocytes. *Eur J Immunol.* 23:2799–2806. [10.1002/eji.1830231112](https://doi.org/10.1002/eji.1830231112).
- Hori K, Hoshino M. 2017. Neuronal migration and AUTS2 syndrome. *Brain Sci.* 7(5):54–60.
- Hsia H-E, Tüshaus J, Brummer T, Zheng Y, Scilabra SD, Lichtenthaler SF. 2019. Functions of “A disintegrin and metalloproteases (ADAMs)” in the mammalian nervous system. *Cell Mol Life Sci.* 76:3055–3081.
- Hu VW, Sarachana T, Kim KS, Nguyen A, Kulkarni S, Steinberg ME, Luu T, Lai Y, Lee NH. 2009. Gene expression profiling differentiates autism case-controls and phenotypic variants of autism spectrum disorders: Evidence for circadian rhythm dysfunction in severe autism. *Autism Res.* 2:78–97.
- Imtaiyaz Hassan M, Shajee B, Waheed A, Ahmad F, Sly WS. 2013. Structure, function and applications of carbonic anhydrase isozymes. *Bioorg Med Chem.* 21:1570–1582.
- Izquierdo-Serra M, Martínez-Monseny AF, López L, Carrillo-García J, Edo A, Ortigoza-Escobar JD, García Ó, Cancho-Candela R, Carrasco-Marina ML, Gutiérrez-Solana LG, et al. 2018. Stroke-like episodes and cerebellar syndrome in phosphomannomutase deficiency (PMM2-CDG): Evidence for hypoglycosylation-driven channelopathy. *Int J Mol Sci.* 19:619–639. [10.3390/ijms19020619](https://doi.org/10.3390/ijms19020619).
- Jack J, Rotroff D, Motsinger-Reif A. 2014. Lymphoblastoid cell lines models of drug response: successes and lessons from this pharmacogenomic model. *Curr Mol Med.* 14:833–840.
- Kim D, Zai L, Liang P, Schaffling C, Ahlborn D, Benowitz LI. 2013. Inosine enhances axon sprouting and motor recovery after spinal cord injury. *PLoS One.* 8(12):e81948. [10.1371/journal.pone.0081948](https://doi.org/10.1371/journal.pone.0081948).
- Koehler K, Malik M, Mahmood S, Gießelmann S, Beetz C, Hennings JC, Huebner AK, Grahn A, Reumert J, Nürnberg G, et al. 2013. Mutations in GMPPA cause a glycosylation disorder characterized by intellectual disability and autonomic dysfunction. *Am J Hum Genet.* 93:727–734.
- Kusch V, Bornschein G, Loreth D, Bank J, Jordan J, Baur D, Watanabe M, Kulik A, Heckmann M, Eilers J, et al. 2018. Munc13-3 Is required for the developmental localization of Ca<sup>2+</sup> channels to active zones and the nanopositioning of Cav2.1 near release sensors. *Cell Rep.* 22:1965–1973.
- Lecca MR, Maag C, Berger EG, Hennet T. 2011. Fibrotic response in fibroblasts from congenital disorders of glycosylation. *J Cell Mol Med.* 15:1788–1796.
- Lecca MR, Wagner U, Patrignani A, Berger EG, Hennet T. 2005. Genome-wide analysis of the unfolded protein response in fibroblasts from congenital disorders of glycosylation type-I patients. *FASEB J.* 19:240–242.
- Lefebvre S, Bürglen L, Reboullet S, Clermont O, Burlet P, Viollet L, Benichou B, Cruaud C, Millasseau P, Zeviani M. 1995. Identification and characterization of a spinal muscular atrophy-determining gene. *Cell.* 80:155–165.
- Liberzon A, Birger C, Thorvaldsdóttir H, Ghandi M, Mesirov JP, Tamayo P. 2015. The Molecular Signatures Database (MSigDB) hallmark gene set collection. *Cell Syst.* 1:417–425.
- Longman C, Brockington M, Torelli S, Jimenez-Mallebrera C, Kennedy C, Khalil N, Feng L, Saran RK, Voit T, Merlini L, et al. 2003. Mutations in the human *LARGE* gene cause MDC1D, a novel form of congenital muscular dystrophy with severe mental retardation and abnormal glycosylation of alpha-dystroglycan. *Hum Mol Genet.* 12:2853–2861.
- López-Gálvez R, de la Morena-Barrio ME, López-Lera A, Pathak M, Miñano A, Serrano M, Borgel D, Roldán V, Vicente V, Emsley J, et al. 2020. Factor XII in PMM2-CDG patients: Role of N-glycosylation in the secretion and function of the first element of the contact pathway. *Orphanet J Rare Dis.* 15:280. [10.1186/s13023-020-01564-9](https://doi.org/10.1186/s13023-020-01564-9).
- Lyons JJ, Milner JD, Rosenzweig SD. 2015. Glycans instructing immunity: The emerging role of altered glycosylation in clinical immunology. *Front Pediatr.* 3:54. [10.3389/fped.2015.00054](https://doi.org/10.3389/fped.2015.00054).
- Marti GE, Kuo MC, Shaw S, Chang CC, Demars R, Sogn JA, Coligan JE, Kindt TJ. 1983. A novel HLA-D/DR-like antigen specific for human B lymphoid cells. Biochemical evidence for similarity to but nonidentity with known HLA-D/DR antigens. *J Exp Med.* 158:1924–1937.
- Martínez-Monseny AF, Bolasell M, Callejón-Póo L, Cuadras D, Freniche V, Itzep DC, Gassiot S, Arango P, Casas-Alba D, de la Morena E, et al. 2019. AZATAX: Acetazolamide safety and efficacy in cerebellar syndrome in PMM2 congenital disorder of glycosylation (PMM2-CDG). *Ann Neurol.* 85:740–751.
- Matthijs G, Schollen E, Bjursell C, Erlandson A, Freeze H, Imtiaz F, Kjaergaard S, Martinsson T, Schwartz M, Seta N, et al. 2000. Mutations in PMM2 that cause congenital disorders of glycosylation, type Ia (CDG-Ia). *Hum Mutat.* 16:386–394.
- Matthijs G, Schollen E, Van Schaftingen E, Cassiman JJ, Jaeken J. 1998. Lack of homozygotes for the most frequent disease allele in carbohydrate-deficient glycoprotein syndrome type 1A. *Am J Hum Genet.* 62:542–550.
- Miller G, Lipman M. 1973. Release of infectious Epstein-Barr virus by transformed marmoset leukocytes. *Proc Natl Acad Sci U S A.* 70:190–194.
- Monticelli M, Ferro T, Jaeken J, Dos Reis FV, Videira PA. 2016. Immunological aspects of congenital disorders of glycosylation (CDG): a review. *J Inher Metab Dis.* 39:765–780.
- Morelle W, Potelle S, Witters P, Wong S, Climer L, Lupashin V, Matthijs G, Gadomski T, Jaeken J, Cassiman D, et al. 2017. Galactose supplementation in patients with TMEM165-CDG rescues the glycosylation defects. *J Clin Endocrinol Metab.* 102:1375–1386.
- Morton DJ, Kuiper EG, Jones SK, Leung SW, Corbett AH, Fasken MB. 2018. The RNA exosome and RNA exosome-linked disease. *RNA.* 24:127–142.
- Mukaigasa K, Tsujita T, Nguyen VT, Li L, Yagi H, Fuse Y, Nakajima-Takagi Y, Kato K, Yamamoto M, Kobayashi M. 2018. Nrf2 activation attenuates genetic endoplasmic reticulum stress induced by a mutation in the phosphomannomutase 2 gene in zebrafish. *Proc Natl Acad Sci U S A.* 115:2758–2763.
- Neuner-Jehle M, Denizot JP, Borbély AA, Mallet J. 1996. Characterization and sleep deprivation-induced expression modulation of dextrin, a novel dendritic protein in rat brain neurons. *J Neurosci Res.* 46:138–151.
- Orvisky E, Stubblefield B, Long RT, Martin BM, Sidransky E, Krasnewich D. 2003. Phosphomannomutase activity in congenital disorders of glycosylation type Ia determined by direct analysis of the interconversion of mannose-1-phosphate to mannose-6-phosphate by high-pH anion-exchange chromatography with pulsed amperometric detection. *Anal Biochem.* 317:12–18.
- Osowski CM, Urano F. 2011. Measuring ER stress and the unfolded protein response using mammalian tissue culture system. *Methods Enzymol.* 490:71–92.
- Parkinson WM, Dookwah M, Dear ML, Gatto CL, Aoki K, Tiemeyer M, Brodie K. 2016. Synaptic roles for phosphomannomutase type 2 in a new *Drosophila* congenital disorder of glycosylation disease model. *Dis Model Mech.* 9:513–527.
- Péanne R, de Lonlay P, Foulquier F, Kornak U, Lefeber DJ, Morava E, Pérez B, Seta N, Thiel C, Van Schaftingen E, et al. 2018. Congenital disorders of glycosylation (CDG): Quo vadis? *Eur J Med Genet.* 61:643–663.
- Perussia B, Ramoni C, Anegón I, Cuturi MC, Faust J, Trinchieri G. 1987. Preferential proliferation of natural killer cells among peripheral blood mononuclear cells cocultured with B lymphoblastoid cell lines. *Nat Immun Cell Growth Regul.* 6:171–188.
- Pokidysheva E, Boudko S, Vranka J, Zientek K, Maddox K, Moser M, Fässler R, Ware J, Bächinger HP. 2014. Biological role of prolyl 3-hydroxylation in type IV collagen. *Proc Natl Acad Sci U S A.* 111:161–166.
- Quintana E, Navarro-Sastre A, Hernández-Pérez JM, García-Villoria J, Montero R, Artuch R, Ribes A, Briones P. 2009. Screening for congenital disorders of glycosylation (CDG): Transferrin HPLC versus isoelectric focusing (IEF). *Clin Biochem.* 42:408–415.
- Radenkovic S, Bird MJ, Emmerzaal TL, Wong SY, Felgueira C, Stiers KM, Sabbagh L, Himmelreich N, Poschet G, Windmolders P, et al. 2019. The metabolic map into the pathomechanism and treatment of PGM1-CDG. *Am J Hum Genet.* 104:835–846.
- Rooney CM, Rickinson AB, Moss DJ, Lenoir GM, Epstein MA. 1984. Paired Epstein-Barr virus-carrying lymphoma and lymphoblastoid cell lines from

- Burkitt's lymphoma patients: Comparative sensitivity to non-specific and to allo-specific cytotoxic responses in vitro. *Int J Cancer*. 34:339–348.
- Ruiz-Lafuente N, Alcaraz-García M-J, Sebastián-Ruiz S, Gómez-Espuch J, Funes C, Moraleda J-M, García-Garay M-C, Montes-Barqueros N, Minguela A, Álvarez-López M-R, et al. 2014. The gene expression response of chronic lymphocytic leukemia cells to IL-4 is specific, depends on ZAP-70 status and is differentially affected by an NF $\kappa$ B inhibitor. *PLoS One*. 9:e109533. [10.1371/journal.pone.0109533](https://doi.org/10.1371/journal.pone.0109533).
- Sasaki K, Yoshida H. 2015. Organelle autoregulation-stress responses in the ER, Golgi, mitochondria and lysosome. *J Biochem*. 157:185–195.
- Shang J, Körner C, Freeze H, Lehrman MA. 2002. Extension of lipid-linked oligosaccharides is a high-priority aspect of the unfolded protein response: Endoplasmic reticulum stress in Type I congenital disorder of glycosylation fibroblasts. *Glycobiology*. 12:307–317.
- Sicari D, Igarria A, Chevet E. 2019. Control of protein homeostasis in the early secretory pathway: Current status and challenges. *Cell*. 8(11):1347–1368.
- Sie L, Loong S, Tan EK. 2009. Utility of lymphoblastoid cell lines. *J Neurosci Res*. 87:1953–1959.
- Subramanian A, Tamayo P, Mootha VK, Mukherjee S, Ebert BL, Gillette MA, Paulovich A, Pomeroy SL, Golub TR, Lander ES, et al. 2005. Gene set enrichment analysis: A knowledge-based approach for interpreting genome-wide expression profiles. *Proc Natl Acad Sci U S A*. 102:15545–15550.
- Tayebi N, Andrews DQ, Park JK, Orvisky E, McReynolds J, Sidransky E, Krasnewich DM. 2002. A deletion-insertion mutation in the phosphomannomutase 2 gene in an African American patient with congenital disorders of glycosylation-Ia. *Am J Med Genet*. 108:241–246.
- Thiesler CT, Cajic S, Hoffmann D, Thiel C, van Diepen L, Hennig R, Sgodda M, Weißmann R, Reichl U, Steinemann D, et al. 2016. Glycomic characterization of induced pluripotent stem cells derived from a patient suffering from phosphomannomutase 2 congenital disorder of glycosylation (PMM2-CDG). *Mol Cell Proteomics*. 15:1435–1452.
- Veerman K, Tardiveau C, Martins F, Coudert J, Girard J-P. 2019. Single-cell analysis reveals heterogeneity of high endothelial venules and different regulation of genes controlling lymphocyte entry to lymph nodes. *Cell Rep*. 26:3116–3131.e5.
- Veiga-da-Cunha M, Vleugels W, Maliekal P, Matthijs G, Van Schaftingen E. 2008. Mammalian phosphomannomutase PMM1 is the brain IMP-sensitive glucose-1,6-bisphosphatase. *J Biol Chem*. 283:33988–33993.
- Verheijen J, Tahata S, Kozicz T, Witters P, Morava E. 2019. Therapeutic approaches in congenital disorders of glycosylation (CDG) involving N-linked glycosylation: An update. *Genet Med*. 22:268–279.
- Wannemacher KM, Wang L, Zhu L, Brass LF. 2011. The role of semaphorins and their receptors in platelets: Lessons learned from neuronal and immune synapses. *Platelets*. 22:461–465.
- Wopereis S, Morava E, Grünewald S, Adamowicz M, Huijben KMLC, Lefeber DJ, Wevers RA. 2005. Patients with unsolved congenital disorders of glycosylation type II can be subdivided in six distinct biochemical groups. *Glycobiology*. 15:1312–1319.